DRFC / CAD

EUR - CEA - FC 1391

Hamiltonian Theory of the Ion Cyclotron Minority Heating Dynamics in Tokamak Plasmas.

A. BECOULET, D.J. GAMBIER, A. SAMAIN

Mars 1990

Hamiltonian Theory of the Ion Cyclotron Minority Heating Dynamics in Tokamak Plasmas.

A. Becoulet, D.J. Gambier, A. Samain.

Association Euratom-CEA sur la Fusion Contrôlée
Centre d'Etudes Nucléaires de Cadarache
13108, St. Paul Lez Durance, France.

submitted for publication in Physics of Fluids B : Plasma Physics

ABSTRACT

The question of heating a tokamak plasma by means of electromagnetic waves in the Ion Cyclotron Range of Frequency (ICRF) is considered in the perspective of large RF powers and in the low collisionality regime. In such case the Quasi Linear Theory (QLT) is validated by the Hamiltonian dynamics of the wave particle interaction which exceeds the threshold of the intrinsic stochasticity. The Hamiltonian dynamics is represented by the evolution of a set of three canonical action angle variables well adapted to the tokamak magnetic configuration. This approach allows to derive the RF diffusion coefficient with very few assumptions. The distribution function of the resonant ions is written as a Fokker Planck equation but the emphasis is put on the QL diffusion instead of on the usual diffusion induced by collisions. Then the Fokker Planck equation is given a variational form from which a solution is derived in the form of a semi analytical trial function of three parameters : the percentage of resonant particle contained in the tail; an isotropic width ΔT and an anisotropic one ΔP. This solution is successfully tested against real experimental observations. Practically it is shown that in the case of JET the distribution function is influenced by adiabatic barriers which in turn limit the Hamiltonian stochasticity domain within energy values typically in the MeV range. Consequently and for a given ICRF power, the tail energy excursion is lower and its concentration higher than that of a bounce averaged prediction. This may actually be an advantage for machines like JET considering the energy range required to simulate the α-particle behaviour in a relevant fusion reactor.

I. INTRODUCTION

Because of its relevance to the achievement of thermonuclear fusion, the Ion Cyclotron Range of Frequency heating of Tokamak plasmas has been extensively studied experimentally[1,2,3,4,5]. Out of the many possible schemes, the minority scenario appears to have the best potential to increase the total plasma energy. In this scenario, the plasma heating is the result of collisions in between a minority population of energetic resonant ions and the bulk plasma. A close look at the energy signal and in particular at the one derived from diamagnetic loop measurements reveals that the wave energy absorption by the resonant ions results in the formation of a strongly anisotropic velocity tail[5,6]. The dynamics of minority ICRF heating is then driven by two antagonistic mechanisms : an anisotrope tail formation for the resonant ions due to the wave particle interaction and an isotrope tail slowing down due to Coulombian processes of collisional relaxation.

The anisotropy in the velocity space is no surprise as the physics of the wave absorption is that of accelerating ions through an increase of their Larmor radius. However a difficulty occurs when it comes to account for the anisotropy in the ICRF power balance. The ICRF heating is a moment of the kinetic equation for the distribution function $f_s(\mathbf{r},v,t)$ of the resonant ion species "s" governed by the equation :

$$\frac{\partial}{\partial t}[f_s] - C[f_s] - Q[f_s] = 0, \qquad [1]$$

in which C is the linearised collision operator of Spitzer[7] and Q the Quasi Linear (QL) RF operator first derived by Kennel and Engelman[8] in a slab geometry. The difficulty comes in [1] from a mutual exclusion of the two operators Q and C. In the case where the RF field is negligible the equation reduces to the Fokker Planck equation $\{\frac{\partial}{\partial t} - C\}[f_s]$. When the operator C is expanded over the parallel velocity ($v_{//}$) and the pitch angle (η), the Fokker Planck equation becomes separable and the Legendre Polynomials[9] form the set of eigen functions in η. On the opposite, when collisions are negligible, the equation reduces to the QL Vlasov equation which in turn can be solved in the phase space when the operator Q is decomposed over a coordinate system built out of the RF resonance lines and their orthogonals. The difficulty originates from the mutual exclusion of these two basis. In the past, the ways to alleviate this difficulty was to consider the RF operator as a

small perturbation[10] so that the decomposition over ($v_{//},\eta$) could continue to hold. This and the flux averaging procedure is what is included in the initial work of Stix[9], from which many other works derive[11,12]. Further developments included in the RF diffusion operator the averaged effect of the trajectories so that resonance localization could be considered[13,14] for both passing and trapped particles. This approach known as the averaged bounce Fokker Planck equation follows essentially the same line of thought and does not yet address the question posed by the RF diffusion operator that is : the basis of description for the Fokker Planck equation is no longer practical in the limit of large RF perturbation (although large the RF amplitude is still small enough to not invalidate the QL plasma response approximation). The question is given so little consideration that when "negative temperature" ($\partial \ln f/\partial E>0$) is found in the analysis of charge exchange signals the possibility that anisotropy may be the cause of it is eliminated without much justifications[14]. So when the anisotropy becomes so pronounced that it has a macroscopic counterpart in the global plasma energy it is the opposite approach that must be taken. In this approach the emphasis is put on the anisotropic nature of the ICRF minority heating and the role of collisions is to insure that energy is back ceded to the bulk plasma. So collisions have only a perturbative effect. As a further approximation the bulk plasma is supposed to be a thermostat so the temperature of each of its constituents (electrons and non resonant ions) is constant. This in turn allows to set to zero all the partial time derivatives so that the velocity distribution function of resonant ions is stationnary. This is what this article addresses. However in situation where the heating dynamics becomes a key factor as in the case of the ignition dynamics the problem could at some expense be solved by a two time scales integration technique : a short time scale where the thermostat constraint is satisfied and at the end of which the energy back ceded to the bulk plasma serves to calculate a new plasma stage which in turn permits to iterate the computation process[15,16].

The analysis presented here is conducted within the frame of the Quasi Linear Theory and it uses the Hamiltonian formalism[17] which was originally developed to derive the ICRF field amplitude in axisymmetric Tokamak plasma configurations (Cf. §.II). The Hamiltonian formulation allows to precisely account for the effect of the particle trajectory on the derivation of the QL RF diffusion coefficient. In that regard the QL diffusion coefficient is derived from first principles. This is a definite advantage of this theory over

the bounce averaged theory where the QL RF diffusion operator is taken from the slab geometry model of Kennel Engelman and then averaged over the trajectory. Another advantage of the Hamiltonian formulation is that in the canonical variables the QL diffusion operator takes a simple form as shown in the annexe. Even though the present work contains very few approximations, it does not address the question of the radial RF induced transport[18]. This transport finds its origin in the loss of invariance of the canonical toroidal angular momentum[19] that mainly occurs due to the banana tip radial drift that ICRF induces. This limitation imposes in turn that the particle remains on a given magnetic surface.

Of course as the present model is built out of the QLT, the QLT needs to be validated. This is the case if there exists some mechanisms that destroy the reversible nature of the wave particle interaction. But as large RF field amplitudes are motivating the present study, the absorption process may possibly involve high energy particles for which the irreversibility mechanisms is no longer insured by collisions. The irreversible processes are reviewed in §.II : the limit above which the Coulomb collisions fail to ergodize the particle phase in between successive passes across the resonance is derived and the existence of multipole resonances, sufficient in number to ergodize the particle trajectory by means of intrinsic stochasticity, is established for the ICRF interaction. As a last step the quasi linear diffusion coefficient are derived from the Hamiltonian formulation of the ICRF interaction. A consequence is that the line of diffusion are drawn in a two dimensional space directed by two non orthogonal vectors; one normalized by the particle energy H and the other by a combination of the particle magnetic moment and the energy P ($P = H - \frac{m}{e}\mu\omega$; ω being the RF frequency).

In §.III the evolution equation for the distribution function of resonant particles is given a variational formulation in which the collisional and the quasi linear terms are explicited as functions of {H,P}. The use of reduction techniques allows to derive a characteristic QL energy which together with the RF diffusion time allows to show that the RF power transferred to the plasma varies like E^2 as expected from a ballistic calculation. Finally a semi-analytical model using simple trial functions is constructed which turns out to reproduce most of the characteristics of the distribution function that are experimentally observed during minority ICRF heating.

II. HAMILTONIAN ANALYSIS OF THE ICRF WAVE PARTICLE INTERACTION

The Hamiltonian formalism is chosen because it makes the action-angle dynamics formally simple[17]. In an axisymmetric unperturbed Tokamak magnetic configuration, the particle trajectory is integrable and described by a set of three action-angle variables $\{J_k,\Phi_k\}$[20] (Cf. Table.I). Its Hamiltonian H_0 depends only on the action variables ($H_0=H_0(J_k)$) and the motion is quasi-periodic, so actions remain constant and angles rotate linearly.

$$\begin{cases} \dfrac{dJ_k}{dt} = -\dfrac{\partial H_0}{\partial \Phi_k} = 0 & , \text{so } J_k = \text{cst.} \\ \dfrac{d\Phi_k}{dt} = \dfrac{\partial H_0}{\partial J_k} = \omega_k(J_n) & , \text{so } \Phi_k = \omega_k(J_n)t + \text{cst.} \end{cases} \qquad [2]$$

Practically, the effect of a low frequency ICRF perturbation is to disrupt this adiabatic behaviour in regions of the phase space where an efficient coupling (i.e. resonances) between fields and particles occurs. In order to identify those regions, the wave Hamiltonian perturbation is expanded as a Fourier series in the Φ_k's :

$$\delta H(J_n,\Phi_n,t) = \sum_{N_k} h_{N_k}(J_k)\, e^{i(N_k\Phi_k+\omega t)} + \text{C.C.} \qquad [3]$$

where the summation extends over the triplet $\{N_1,N_2,N_3\}$.

For a given triplet $\{N_k\}$ a resonant interaction takes place when $h_{N_k} \neq 0$ and when the phase of the perturbation is stationary along the unperturbed trajectory :

$$\Omega(J_n) = \sum_k N_k\omega_k(J_n) + \omega = 0 \qquad [4]$$

The latter, in the vectorial phase space $\{\{J_k\}=\{0\}+\vec{OJ};\ \vec{J}=\vec{OJ}\}$, defines a resonance surface labelled by the N_k's : $S_R(N_k)$. Let's assume a single resonant surface, an hermiticity of the h_{N_k}'s coefficients and an almost independence of the h_{N_k}'s with N_k; then δH writes $\delta H = s(J_k)\cos(N_k\Phi_k+\omega t)$ with $s(J_k) = 2h_{N_k}$. The time evolution of the J_k's is given by the Hamilton's equations : $\dfrac{d\vec{J}}{dt} = \vec{N}\, s(J_k)\, \sin(\sum_k N_k\Phi_k+\omega t)$. So the motion occurs along the vector $\vec{N}$ and is represented by the set $\{\{J_k\} = \{J_{k,R}\} + \vec{N}\lambda;$

$\varphi = \sum_k N_k\Phi_k+\omega t\}$; $\{J_{k,R}\}$ being the point on the resonance surface $S_R(N_k)$ associated to the unperturbed motion. Then the equation that governs the perturbed particle motion is :

$$\frac{d\lambda}{dt} = s(J_k)\ \sin(\varphi).$$

This motion derives from an invariant energy principle which involves the curvature of the unperturbed Hamiltonian :

$$\alpha = N_i N_j \frac{\partial^2 H_0(J_{k,R})}{\partial J_i \partial J_j} = \frac{\partial^2 H_0(J_{k,R})}{\partial \lambda^2} \qquad [5]$$

taken along the direction of the $\vec{N}$ vector and on the resonance surface $S_R(N_k)$. The invariant is : $W = \frac{1}{2}\alpha\lambda^2 + s(J_{k,R})\cos\varphi$. So the motion in the (λ,φ) space is identical to the motion of a particle trapped in a wave potential well. The shape of the iso-W lines has an island-like structure[20] (Fig.1) and the separatrix between the trapped and the circulating domains verifies the equation: $|W| = s(J_{k,R})$.

However there is more to the present approach which is the possibility for trajectories to interfere. These interferences result from the existence of a set of resonant trajectories and may cause intrinsic stochasticity[22] to occur. Indeed to Eq.[4] corresponds a set of trajectories $\{J_{Ri}\}$ which when represented as surfaces in the (λ,φ) space are distant of $\Delta\Omega_R = (\Delta N_k)\omega_k$ (Fig.2). Correspondingly, the island width counted in Ω is $\Delta\Omega_I = 4\sqrt{s\alpha}$. If $\Delta\Omega_R < \Delta\Omega_I$, then overlapping of islands starts to occur (Fig.3). The regular behaviour of the perturbed trajectories is destroyed and stochastic domains between resonance surfaces[24] are created. So intrinsic stochasticity is insured when the Chirikov parameter $S = \Delta\Omega_I/\Delta\Omega_R$ is well in excess of 1. In the case of the ICRF wave particle interaction in the Tokamak geometry, stochasticity is triggered by overlapping of nearby resonances (Cf. Table II) but resonance overlapping of harmonics of the gyrofrequency never occurs.

On the overall the effect of stochasticity on the particle trajectory is twofold : the perturbed trajectory is no longer confined around the resonance surfaces and the associated phase is chaotic (Fig.3). Therefrom in a phase space domain where the wave-particle resonant interaction is effective ($h_{N_k} \neq 0$) and where the density of resonance

surfaces is large, the process associated to the particle-wave interaction is diffusive, thereby validating the QLT. The method of analysis amounts to select the set of action-angle variables relevant to the physical situation, to calculate the respective positions of resonance surfaces and the associated h_{N_k}'s, to derive the curvature of the unperturbed Hamiltonian, to evaluate the stochasticity parameter and finally to construct a Poincaré mapping to check the onset of stochasticity.

A. ACTION ANGLE VARIABLES FOR PASSING AND TRAPPED PARTICLES

The particle trajectory is described within the frame of the adiabatic theory[24]; the guiding center $\vec{x}_g$ is labelled by $\{R,r_g,\phi,\theta\}$ and the gyromotion by $\{\rho_c,\phi_c\}$; R,r_g,ρ_c are respectively the major, minor and gyro radii; ϕ,θ are the angles around the major axis and the magnetic axis and ϕ_c is the gyro angle (Fig.4).

The constant set of canonical actions $\{J_k\}$ which specifies the unperturbed particle trajectory is in correspondence with the three adiabatic invariants[22] $\{\mu,H,\mathcal{P}_\phi\}$: the particle magnetic moment $\mu = \frac{mv_\perp^2}{2B}$; the total particle energy $H = \frac{1}{2} mv_{//}^2 + \mu B$; the toroidal angular momentum $\mathcal{P}_\phi = e\Psi_P + mv_\phi R$, with indices $\perp$ and $//$ standing for the perpendicular and the parallel directions to the total magnetic field $\vec{B}$, Ψ_P for the poloidal magnetic flux and v_ϕ for the velocity in the toroidal direction. An analytic expression[25] of the approximated J_k's is being written in Table I where it may be noticed that the magnetic surface appears only in J_3 through the poloidal flux Ψ_P.

In the case of interest, collisions mainly induce a diffusion in $v_{//}$ and thereby in J_2 while the diffusion induced by the RF field takes place in the bi-dimensional space $\{J_1,J_2\}$. There is however the possibility of an RF diffusion in J_3 which amounts to a radial diffusion through Ψ_P. In this work it is not considered on the ground that whatever the anomalous diffusion induced by the overall plasma equilibrium may be, it always dominates the radial transport and therefore that the RF correction is not bound to change this situation. This is further confirmed experimentally when the degradation of the overall confinement time appears to depend on the total coupled power and not on the type of the auxiliary heating source[5]. If the RF induced radial transport were however to be considered, it would increase the diffusion space dimension by one to make it to reach three. The distribution function would become dependent on three parameters which make the problem three-dimensional and consequently almost untractable. The attempt

previously made[19] to account for the RF radial diffusion was to consider the very first terms in the development of J_3 so that the corrections in both $\frac{r_g}{R_0}$ and ρ_c were neglected. In this case the radial diffusion reduces to a diffusion in $v_\perp$ which in turn accounts for a motion of the banana tip towards the low field side. But in this process the diffusion only occurs along the same magnetic surface Ψ_P. Stricto sensu it cannot be considered as a radial diffusion.

On the other hand, the set of canonical angles $\{\Phi_k\}$ resulting from the integration of the unperturbed trajectory for a given set $\{J_k\}$, specifies :

(i) the gyrophase ϕ_c through $\phi_1 = \phi_c - \Theta(\mu,H,\mathcal{P}_\phi)$;

(ii) the drift surface in the poloidal and toroidal directions through ϕ_2 and ϕ_3 respectively (Cf. Table I).

The value $\omega_1(J) = d\phi_1/dt$ is the time averaged value along the trajectory of $\omega_c(x_g)$ and the difference $\omega_c - \omega_1$, of order $\omega_c r_g/R_0$, exhibits a large variation rate. Because of the axisymmetry, the relation of θ and ϕ in terms of ϕ_2 and ϕ_3 writes : $\theta = \varepsilon\phi_2 + \hat{\theta}(\phi_2)$; $\phi = \phi_3 + q(\Psi_P)\,\hat{\theta}(\phi_2) + \hat{\phi}(\phi_2)$; where $\hat{\theta}(\phi_2)$ and $\hat{\phi}(\phi_2)$ are 2π-periodic functions of ϕ_2 ($\varepsilon = 1$ for passing particles, resp. 0 for trapped particles and $q(\Psi_P)$ is the safety factor). Therefore, the trajectory is completed within the time duration $2\pi/\omega_2$: $\omega_2(J) = d\phi_2/dt$, allowing to restrict the study over this time period.

B. EFFECTIVE ICRF RESONANCES

In the ICRF heating scheme, the electromagnetic power is carried by a fast wave polarized in the extraordinary mode. In the plasma core, the wave is a compressional Alfven wave with an electric field and a wave vector predominantly perpendicular to the magnetic field : $k_\perp = \omega/c_A$. The pulsation ω is imposed by the RF generator and the coupling launcher allows a discrete toroidal mode spectrum in k_ϕ : $k_\phi = N/R$. The compressional wave is written in the gauge $[A_\perp,\psi=0]$ and the perturbed Hamiltonian of the form : $\delta H = -e\, V_\perp A_\perp(\vec{x}_g+\vec{\rho}_c)$ with $\vec{V}=\frac{\partial H_0}{\partial \vec{p}}$.

Up to this point the Hamiltonian representation is not equivalent to the classical ballistic approach[9,21]. From a ballistic point of view the wave particle resonant coupling occurs at some point $\vec{x}^*_g$ along the guiding center trajectory, where the particle

gyrophase matches the wave phase: $\omega + \omega_c(\vec{x}^*_g) = 0$. So the ballistic resonant condition is not like Eq.[4]. To be equal requires that $\omega_c(\vec{x}^*_g) = N_k\omega_k(J_{k,R})$ is satisfied. This apparent discrepancy comes from the fact that in the action angle representation the resonance condition is twofold : the stationarity of the phase which writes $\Omega(J_k)=0$ and the non vanishing value of the Fourier coefficient $h_{N_k}(J_k)$. Consequently a method to derive the actual $h_{N_k}(J_k)$ value needs to be devised.

The last expression of δH when Taylor expanded around $\vec{x}_g$ takes the form of a Fourier series in $\exp\{ip\phi_c\}$:

$$\delta H = \sum_p h_p(\mu,H,\vec{x}_g)\, e^{i(p\phi_c+\omega t)} + C.C. \qquad [6]$$

where $h_p(\mu,H,\vec{x}_g)$ takes the following form :

$$h_p(\mu,H,\vec{x}_g) = \frac{(-i)^p e\rho_c\omega_c}{2}\left\{ J_{p-1}(k_\perp\rho_c)\, A_- + J_{p+1}(k_\perp\rho_c)\, A_+ \right\} \qquad [7]$$

if for simplicity the perpendicular wave vector is introduced in place of partial derivatives and $A_\pm$ is the complex polarisation potential.

At this stage the expression of the h_{N_k}'s coefficient may be worked out. If we compare Eq.[6] to the action-angle expression of δH (Eq.[3]) and consider a launched toroidal mode N, it is apparent that : the h_{N_k}'s components will vanish if $N_3 \neq N$ and if $N_1 \neq p$. So we only need to consider the cases $h_{N_1=p,N_2,N}$. If we further recall that because of the axisymmetry an unperturbed trajectory is completed when the canonical poloidal angle Φ_2 is varied within 2π, the expression of the h_{N_k}'s can be derived multiplying δH by $e^{-i(N_k\Phi_k+\omega t)}$ as would normally be done for a Fourier series but performing an integration only in Φ_2 over 2π :

$$h_{N_1=p,N_2,N} = \int_0^{2\pi} \delta H\, e^{-i(N_k\Phi_k+\omega t)}\, \frac{d\Phi_2}{2\pi} \qquad [8]$$

If the expression [6] is introduced in place of δH in the integral [8], the argument in the exponential function becomes : $p(\phi_c - \Phi_1) - N_2\Phi_2 - N\Phi_3$. The phase mixes the canonical angle variables Φ_k and the particle gyrophase ϕ_c which depends upon the guiding centre

trajectory in the real space $\phi_c = \int \omega_c(\vec{x}_g)dt$. However the angle variables Φ_k are linear functions of time and the phase can be written $p\Theta - N_2\omega_2 t - N\omega_3 t$, where an arbitrary constant has been omitted. Finally we can change variables from Φ_2 to the running time variable "t" because the integration needs only to be performed over Φ_2, with the transformation rule $d\Phi_2 = \omega_2(J_k)\, dt$, so :

$$h_{N_1=p,N_2,N} = \frac{\omega_2}{2\pi} \int_0^{2\pi/\omega_2} h_p\, e^{ip\Theta - i(N_2\omega_2 + N\omega_3)t}\, dt\,. \qquad [9]$$

As mentioned, Θ has a variation rate ($d\Theta/dt = \omega_c - \omega_1 \approx \omega_c r_g/R_0$) typically much larger than the one of h_p. Therefore the integral will be non vanishing if along the trajectory there exists points where the phase is stationary, namely when :

$$p\omega_c(\vec{x}_g^*) = p\omega_1 + N_2\omega_2 + N\omega_3 \qquad [10]$$

The number ΔN_2 of effective resonances is then defined by the number of N_2 verifying the previous relation. As an example for passing particles $N_2 \approx p r_g \omega_c/R_0\omega_2$ (Table II) and $\omega_c(\vec{x}_g^*)$ varies by $2\omega_1 r_g/R_0$ over a complete revolution, thereby $\Delta N_2 = 2p\,\frac{\omega_1 r_g}{\omega_2 R_0}$.

C. CYCLOTRON RESONANCE EFFECT PER PASS FOR PASSING AND TRAPPED PARTICLES : STEEPEST DESCENT TECHNIQUE

In the expression [9], each resonance crossing produces a net exchange of energy between the wave and the particle. Considered for itself the saddle point at which the resonance occurs has a characteristic scale $\lambda_c = v_{//}/\sqrt{p v_{//} \nabla_{//} \omega_c}$. Along the trajectory, two situations may be encountered (Fig.4). The first one is when the resonance points are far removed and the variation scale of h_p is larger than λ_c, then the integrand involves an isolated first order saddle point so that the classical steepest descent technique is applicable[26]. Note that when the variation scale is much shorter than λ_c then h_p can be decomposed over WKB waves in the parallel direction which shifts the resonant conditions[17] by $k_{//}v_{//}$. Around the resonance point $\vec{x}_g^*$ the following quantity may be developed :

$$\begin{cases} \vec{x}_g = \vec{x}^*_g + v_{//}(t-t^*)\dfrac{\vec{B}}{B} \\ p\Theta-(N_2\omega_2+N\omega_3)t = p\Theta(\vec{x}^*_g)-(N_2\omega_2+N\omega_3)t^* + \frac{1}{2}\, p\dot{\omega}_c(\vec{x}^*_g)\,(t-t^*)^2 \\ \dot{\omega}_c(\vec{x}_g) = v_{//}\nabla_{//}(\omega_c(\vec{x}_g)). \end{cases}$$

The phase evolution around the resonance point is then parabolic as sketched in Fig.5(a). The contribution to the integral of $h_{N_1=p,N_2,N}$ in [9] is :

$$\delta h^{I}_{N_1=p,N_2,N} = \frac{\omega_2}{2\pi}\sqrt{\frac{2\pi}{pv_{//}\nabla_{//}(\omega_c(\vec{x}^*_g))}}\, h_p(\mu,H,\vec{x}^*_g)\,\left\{e^{ip\Theta(\vec{x}^*_g)-i(N_2\omega_2+N\omega_3)t^*}\right\} \qquad [11]$$

The second situation is met when two consecutive resonance points are closer to each other than λ_c and so the integrand involves two relevant isolated saddle points[26]. This is the case for banana trajectory when the banana tip is close to the resonance points. This last situation requires to develop the phase at the next order in time as $v_{//}$ vanishes and is best achieved when the development is performed around the time $\underline{t}$ at which the particle reaches the banana tip. Then we have the following developments :

$$\begin{cases} \vec{x}_g = \vec{\underline{x}}_g + \frac{1}{2}\,\dot{v}_{//}(t-\underline{t})^2 \\ \Phi(t) = p\Theta-(N_2\omega_2+N\omega_3)t = \Phi(\underline{t}) + p(\omega_c(\vec{\underline{x}}_g)+\omega)(t-\underline{t}) + \frac{1}{6}\,p\,\ddot{\omega}_c(\vec{\underline{x}}_g)(t-\underline{t})^3 \end{cases}$$

the phase evolves then as a cubic function of the position as sketched on Fig.5-(b) and this leads to a contribution to the $h_{N_1=p,N_2,N}$ integral of the form :

$$\delta h^{II}_{N_1=p,N_2,N} = \omega_2\sqrt[1/3]{\frac{2}{p\,\ddot{\omega}_c(\vec{\underline{x}}_g)}}\,\mathrm{Ai}(z)\, h_p(\mu,H,\vec{\underline{x}}_g)\,\left\{e^{i\Phi(\underline{t})}\right\} \qquad [12]$$

where $z = \sqrt[1/3]{\dfrac{2}{p\,\ddot{\omega}_c(\vec{\underline{x}}_g)}}\; p\,(\omega_c(\vec{\underline{x}}_g)+\omega)$ is the Airy function argument and the expression for the second time derivative of ω_c is $\ddot{\omega}_c(\vec{\underline{x}}_g) = -\dfrac{v_{//}(\theta=0)\omega_2 r_g}{qR_0^2}\,\omega_c(\vec{\underline{x}}_g)\sin(\vec{x}_g) > 0$. The case where the banana tip is tangent to the cyclotron resonance surface

find in this formalism a simple solution which in particular does not lead to a singularity in z as $Ai(z = 0) = 3^{-2/3}/\Gamma(2/3)$.

On the overall the behaviour of $\left|\delta h_{N_k}\right|$ as a function of the distance of the banana tip to the cyclotron resonance when measured in angles is represented in figure 6.

E. QUASI LINEAR ICRF HEATING

If each resonance point met along the particle trajectory leads to an exchange in between wave and kinetic energies, the sign of the exchange depends upon the exponential phase factor. To obtain a net transfer of wave energy, the successive values of $\delta h_{N_1=p,N_2,N}$ have to add in modulus square so that the following relations hold :

$$\left|h^{I}_{N_1=p,N_2,N}\right|^2 = \sum_{\vec{x}^*_g} \frac{\omega_2^2}{4\pi^2} \left|\frac{2\pi}{pv_{//}\nabla_{//}(\omega_c(\vec{x}^*_g))}\right| \left|h_p(\mu,H,\vec{x}^*_g)\right|^2 \qquad [13]$$

$$\left|h^{II}_{N_1=p,N_2,N}\right|^2 = \sum_{\vec{x}_g} \omega_2^2 \left|\frac{2}{p\dot{\omega}_c(\vec{x}_g)}\right|^{2/3} |Ai(z)|^2 \left|h_p(\mu,H,\vec{x}_g)\right|^2 \qquad [14]$$

while for the fundamental heating scenario and at lowest order in ρ_c the $h_1(\mu,H,\vec{x}_g)$ value reduces to :

$$\left|h_1(\mu,H,\vec{x}_g)\right| = \frac{|e|v_\perp}{2\omega}|E|. \qquad [15]$$

That is however possible only if the successive values taken by the phase $\Phi(t^*)$ or $\Phi(t)$ are random, i.e. if the Random Phase Approximation (RPA) is valid. So ICRF wave heating to take place requires that the phase of the particle relative to the wave has diffused in between two successive resonance crossings. If the decorrelation process is diffusive, the phase trajectory ϕ ($\phi=\int\Omega dt$) becomes a random variable because the frequency Ω itself diffuses. The law of diffusion is $(\delta\Omega)^2 = \langle(\Delta\Omega)^2\rangle\,\delta t$, so $\delta\phi$ evolves like $\delta\phi=\int\delta\Omega dt$. On the other hand the characteristic diffusion time τ_L is defined as the duration after which the phase has varied by one radian. So τ_L satisfies to $\tau_L\delta\Omega=1$ and therefore $\tau_L=\langle(\Delta\Omega)^2\rangle^{-1/3}$. This in turn allows to further determine a condition for the diffusion to be efficient, that τ_L be much shorter than the characteristic period of the

phenomenom in concern[27]. Applied to the Tokamak configuration, the trajectory period is $\frac{2\pi}{\omega_2}$ and so the efficiency condition amounts to $\tau_L \ll \frac{2\pi}{\omega_2}$.

The diffusion that collisions induce is essentially a diffusion in $v_{//}$. As $v_{//}$ appears in the canonical action J_2 the diffusion is also in J_2 and $\delta J_2 \approx J_2 \sqrt{\frac{t}{\tau_{coll}}}$. Then the total frequency varies as $\delta\Omega \approx N_2 \frac{\partial \omega_2}{\partial J_2} \delta J_2$ and as the resonance condition amounts to $N_2 \approx \frac{r_g \omega}{R_0 \omega_2}$ the diffusion occurs over $\tau_L \approx [\sqrt{\tau_{coll}}\, R_0/\omega r_g]^{2/3}$. The collision diffusion efficiency then amounts to the condition :

$$\left[\frac{q r_g}{\rho_c}\right]^2 \frac{qR}{\lambda_{coll}} = S_{coll} \gg 1, \qquad [16]$$

verified for $T \ll 20$ keV for the Table II parameters with $T_e = T_i$.

In the case of diffusion induced by intrinsic stochasticity[20], S must exceed 1. To derive its expression, the curvature of the unperturbed Hamiltonian must be explicited, i.e $\alpha = N_i N_j \frac{\partial \omega_i}{\partial J_j}$. As $\Delta\Omega_R = \omega_2$ and as for passing particles $\alpha \approx \frac{(N+N_2/q)^2}{mR_0^2}$, S writes in this case :

$$S = \frac{4q}{v_{//}}\left(N + \frac{N_2}{q}\right)\sqrt{\frac{2ev_\perp |E|}{m\omega\sqrt{\pi \sin\theta^* \Delta N_2}}} \qquad [17]$$

With the parameter set of Table II the following domains of applicability may be derived : for $T < 10$ keV, $S_{coll}/S > 1$ so collisions are preponderant; for 10 keV $< T < T_B = 800$ keV, $S > 1$ so stochasticity is dominant.

The expression of S is a decreasing function of the particle energy. This comes from the fact that the distance between resonant surfaces increases more rapidly with energy than it does with the h_{N_k}'s and that rules out any beneficial energy dependance. So there exists an upper limit in energy called the adiabatic barrier[21] above which diffusion ceases to be effective ($T > T_B$ with the Table II parameters). However, due to the N antenna spectrum, the adiabatic barrier can be made very large. For a non integer q value, the resonant surfaces of the family $\{1, N_2, N\}$ fall in between the one of

the family $\{1,N_2,N'\}$. So the distance in between two successive surfaces is effectively reduced. For example if $N'=N+1$, the distance may be made less than ω_2 when $|\Delta N_2+q|<1$. But to verify the onset of stochasticity requires now to perform a Poincaré mapping, which here amounts to plot the successive values taken by λ after each trajectory period, i.e.versus ϕ_2 (Fig.7). It can then be observed that the RPA is valid over a larger temperature range, provided the N antenna spectrum is sufficiently rich.

Finally, the energy domain associated to induced intrinsic stochasticity diffusion is appreciably extended for trapped particles. The reason lies in the fact that the stochastic parameter associated with passing and trapped particles are almost equal when they have the same $v_{//}$ in the resonance zone ($\vec{x}_g=\vec{x}^*_g$). But belonging to different classes, the trapped particle perpendicular energy is not bounded as for the passing particle where $E_\perp(0) \leq \frac{R}{2r} E_{//}(0)$.

F. QUASI LINEAR LINES OF RF DIFFUSION

As aforementioned the motion around an insulated resonance surface occurs along the vector $\vec{N}$ that enters into the relation : $\vec{J} = \vec{J}_R + \vec{N}\lambda$. Then the particle motion ripples around the resonance surface $\vec{J}_R$ and so the particle explores the J_{Rk}'s neighbourhood in the phase space. If there exists a family of resonances $\{\vec{J}_{Ri}\}$ and that the resonant domains greatly overlap, the particle exploration is no longer constrained by one resonance only. Following one $\vec{N}_i$ vector it may enter the next resonant domain and its motion will continue along $\vec{N}_{i+1}$ and so on. The particle phase in all this process is random and therefrom the wave-particle interaction results in a unidimensional diffusion along the lines of $\vec{N}$-vectors. This in principle is not absolutely rigorous. Suppose that the wave spectrum is made of one toroidal mode ($N_3 = N$), then the diffusive lines are correctly defined as depicted on figure 8. It can be shown however that there exists still a small diffusion along the resonance surfaces themselves. This diffusion corresponds to a non-symmetrical particle motion in between two resonant surfaces[28]. For example in one direction the particle follows the direction $\{1,N_2,N\}$ and returns along the direction $\{1,N_2+1,N\}$ (Fig.9-a). This possibility would invalidate the principle of reciprocity presented in the annexe and is consequently ignored. A diffusion of the same kind may also be induced when the toroidal N spectrum excited by the antenna is large. That give birth to a set of resonance directions for each J_R surface as the direction is now defined by

the set of doublets (N_2,N_3) which verify the resonance relation [4]. This should in principle lead to a stronger diffusion mechanism (Fig.9-b) along the resonance surfaces and imply that none of the J_{Rk}'s is a strict invariant. This possibility has not been however explored further and the $\vec{N}$-vector lines will from now on be considered as a good representation to study the quasi linear diffusion.

The lines of diffusion are governed by the following set of equations (the J_3 variation is here introduced only to preserve the generality of the demonstration) :

$$\frac{dJ_1}{N_1} = \frac{dJ_2}{N_2} = \frac{dJ_3}{N_3} = d\lambda$$

while using the resonance relation the particle energy W evolves like :

$$dW = \omega_k dJ_k = (N_k\omega_k)\, d\lambda = -\,\omega\, d\lambda = -\,\frac{\omega}{N_1}\, dJ_1.$$

Applied to the minority heating scheme ($N_1 = 1$), the characteristics of the diffusion lines are represented by the equation :

$$W = -\,\omega J_1 + cst. \qquad [18]$$

This expression shows that the quasi linear diffusion induced by ICRF heating is essentially anisotropic and should be consider as such (note that the same equation is derived from the bounce averaged QLT[14]). The characteristics are straight lines in the ($W,\omega J_1$) space (Fig.10). In ($W,\omega J_1$), only the quadrant ($W>0$, $\omega J_1<0$) corresponds to the physical domain. The line $W = -\omega J_1$ defines the limit under which there is no intersection of the banana trajectory and the cyclotron resonance while the equation $W = -\,b\omega J_1$, where b is the ratio of the gyrofrequency to the RF frequency evaluated at $\theta=0$, defines the limit under which there is no possible trajectory. Finally the direction $P = W + \omega J_1$ defines the direction orthogonal to the line of diffusion. As a remark it may be observed that because the ICRF diffusion process is associated with a perpendicular velocity increase at the resonance location, the parallel velocity at that location remains constant. This particularity favours the use of the variable $v_{//}(\vec{x}_g=\vec{x}^*_g)$ (cf IV: $v_{//}(\vec{x}_g=\vec{x}^*_g) = \sqrt{2P/m}$).

In the real space it is convenient to represent the particle trajectory velocity by its value taken at times where the particle crosses the equatorial plane ($\theta = 0$), hereafter

referred as 0. If the diffusion lines are projected onto the velocity space $\{v_{//0}, v_{\perp 0}\}$, they become hyperbolas (Fig.11) because the parameter b which enters in the diffusion line characteristics is smaller than 1 when the resonance surface intercepts the drift surface. Equation [18] writes :

$$v_{//0}^2 + \left(1 - \frac{1}{b}\right) v_{\perp 0}^2 = \text{cst.} \qquad [19]$$

The asymptotic direction for the RF diffusion lines is defined by : $\frac{v_{\perp 0}}{v_{//0}} = \sqrt{\frac{(-\omega_{c0})}{\omega + \omega_{c0}}}$, while the last equation corresponds to the case where the resonance surface is tangent to the point $\theta = 0$. It can also be noticed that the line $\frac{v_{\perp 0}}{v_{//0}} = \sqrt{\frac{2r_g}{R_0}}$, which limits the two domains of trapped and passing particles, intersects the diffusion lines showing that ultimately all resonant particles would run along the asymptotic direction and end in the trapped domain if there was no collision to drag them out.

III. VARIATIONAL FORM OF THE FOKKER PLANCK EQUATION

From now on the kinetic equation for the evolution of the distribution function of the resonant ions will be referred as the Fokker Planck equation. This is justified (Cf. Annexe) if we consider that the ICRF induces a quasi linear diffusion which, in terms of the action angle variables, amounts to performed an averaging over the angle variables. Then the QL expression of the ICRF diffusion operator writes :

$$Q(\bar{f}) = \frac{1}{2}\frac{\partial}{\partial J_i}\left(\left\{ 4\pi \sum_{N_k} N_i N_j \left| h_{N_k} \right|^2 \delta(N_k\omega_k + \omega) \right\} \frac{\partial \bar{f}}{\partial J_j} \right) \qquad [20]$$

where $\bar{f} = \int f(J_k, \Phi_k, t)\, d^3\Phi_k/(2\pi)^3$ is the phase averaged distribution function. At this point it is important that a comparison be made between the bounce Fokker Planck and the present approach. The bounce average method[29] has been devised to take account of the particle trajectory effects and in particular of banana particles for which the time spent within the resonance may increase drastically. The present approach may be viewed as an extension of the bounce average method in the sense that the detail of the localized resonant interaction is considered with very few approximations. The reason for the low number of approximations must be found in the Hamiltonian representation of the ICRF interaction. Only in this representation the complexity of the guiding centre trajectory can

be made formally simple and the detail of the ICRF interaction can be unfolded easily (Cf. §.II where the algebra amounts to perform integrals using the steepest descent method). So the present Hamiltonian formulation of the ICRF heating generalizes the previous methods.

The Quasi Linear RF diffusion operator is essentially anisotropic and it follows characteristics which are simple straight lines in the $\{W,\omega J_1\}$ space. In order to respect the natural space for the ICRF diffusion study, the Fokker Planck equation is written in that space rather than in the $\{v_{//},v_\perp\}$ space. The vector basis will be directed by two non orthogonal unit vectors $\vec{h}$ and $\vec{p}$, while H=W and $P = W + \omega J_1$. This decomposition not only emphasizes the role of the ICRF diffusion but also respects the structure of the collisional operator $C(f)$. Indeed $C(f)$ mainly produces a diffusion in P and an isotropic drag in P and H.

In order to find the solution of the Fokker Planck equation :

$$\frac{\partial \bar{f}}{\partial t} = Q(\bar{f}) + \int C(f)\,\frac{d^3\Phi_k}{(2\pi)^3}, \qquad [21]$$

the Fokker Planck equation is considered to be the Euler equation of a functional $\boldsymbol{L}$, extremal for all variation of a trial function $\bar{f}'(J_k)$. The $\boldsymbol{L}$ functional is built out of equation [21] and takes the form of an integral over the J_k's. The integration domain is bounded by the adiabatic barriers above which the quasi linear analysis fails. The $\boldsymbol{L}$-expression writes :

$$\boldsymbol{L} = \int d^3J_k \frac{\partial \bar{f}}{\partial t}\,\bar{f}'(J_k) - \boldsymbol{L}_{QL} - \boldsymbol{L}_{Coll} \qquad [22]$$

with $$\boldsymbol{L}_{QL} = \frac{1}{2}\int d^3J_k \frac{\partial}{\partial J_i}\left(\left\{4\pi \sum_{N_k} N_i N_j \left|h_{N_k}\right|^2 \delta(N_k\omega_k+\omega)\right\}\frac{\partial \bar{f}}{\partial J_j}\right)\bar{f}'(J_k) \qquad [23]$$

and $$\boldsymbol{L}_{Coll} = \int d^3J_k \frac{d^3\Phi_k}{(2\pi)^3}\, C(f(J_k,\Phi_k,t))\;\bar{f}'(J_k)) \qquad [24]$$

In order to carry out the $\bar{f}$ solutions, some algebra needs to be perform so that $\boldsymbol{L}$ can be written in a form suitable for the physical and the numerical analysis. In this article only

the physical analysis will be carried out leaving the complete numerical analysis to another work. The present variational formulation is however constructed for a usage of finite element techniques so that the numerics reduces to an eigen value problem, i.e. a matrix inversion[17].

A. THE QUASI LINEAR PART OF THE FUNCTIONAL L

The equation [23] which defines the QL functional can be integrated by part so that the derivative operator $N_k\frac{\partial}{\partial J_k}$ acts on both $\bar{f}$ and $\bar{f}'$. So the derivation is performed along the $\vec{N}$ vector thereby along the diffusion lines. But as the particle is supposed to remain on a given magnetic surface, J_3 is constant and the derivative operator reduces in the $\{H,P,J_3\}$ space to a derivation along H. It takes the form of $-\omega\frac{\partial}{\partial H}$.

The sum over the N_k's in [23] involves $|h_{N_k}|^2\,\delta(\omega+N_k\omega_k)$. The quasi linear diffusion is supposed to be effective in the overall phase space accessible to $\Omega(J_k)=0$, which in our case corresponds to the overall phase space accessible when N_2 is varied, the distance in Ω between two adjacent resonant surfaces being ω_2. On the other side the h_{N_k}'s have a weak dependence in N_2 and may be considered to a large extend as constant over the phase space $\Omega(J_k)=0$. Therefore the sum reduces to $\sum_{N_2}\delta(\omega+N_k\omega_k)=1/\omega_2$ and L_{QL} takes the form :

$$L_{QL} = -\int dP dH dJ_3\, 2\pi\,\omega\,\frac{|h_{N_k}|^2}{\omega_2^2}\frac{\partial\bar{f}}{\partial H}\frac{\partial\bar{f}'}{\partial H} \qquad [25]$$

From that expession it is possible to apply the reduction technique which in turn allows to find a RF quasi linear characteristic energy $\tilde{H}$ so that with $P = p\tilde{H}$, $H = h\tilde{H}$, eqs.[12] and [14], L_{QL} can be written :

$$L_{QL} = \frac{\tilde{H}^2}{\omega}\int dp dh dJ_3\,\sigma^{P,T}\frac{h\text{-}p}{\sqrt{p}}\frac{\partial\bar{f}}{\partial h}\frac{\partial\bar{f}'}{\partial h} \qquad [25]$$

with $\sigma^P = 1$ for passing particle trajectory and $\sigma^T = 2$ for trapped one's.

The characteristic energy itself is of the form :

$$\tilde{H} = \sqrt[2/3]{\frac{qR_0}{r_g}R_0E^2\sqrt{\frac{m}{2}}\frac{eb}{B_0\sin\theta^*}} \qquad [26]$$

The characteristic power $\tilde{P}_{RF}$ transferred to the resonant species is the ratio of $\tilde{H}$ to the QL diffusion time τ_L induced by the RF field. The QL diffusion coefficient is proportional to E^2 and so τ_L to $E^{-2/3}$. Therefore $\tilde{P}_{RF}$ is proportional to E^2 and by means of consequence to the power carried by the wave.

B. THE COLLISIONAL PART OF THE FUNCTIONAL *L*

The phase integration met in L_{Coll} can be simplified when the following remarks are made : the distribution function f and the collision operator C are function of the slow variables of the adiabatic theory and thereby not function of the gyrophase ϕ_c or of the gyro canonical angle Φ_1; because of the axisymmetry f is not a function of Φ_3 and finally the trajectory being completed when Φ_2 is varied by 2π, f is 2π-periodic in Φ_2. If we further neglect the effect of toroidicity on the collision operator then C is independent of Φ_3 as well. This last approximation is also found in the bounce averaged theory and is strictly valid only for large aspect ratio Tokamak.

The expression of $C(f)$ is usually written[7] using the velocity modulus (v), the pitch angle (η) and the current poloidal angle (θ). It comprises three terms : one which, captures most of the physics of the slowing down of a test particle in a background of ions and electrons, contains a parallel drag due to collisions with ions or electrons or both depending upon the test particle energy (at high energy the drag is mainly driven by collisions with electrons and conversely) and contains also a part representing a perpendicular energy isotropisation or diffusion. The second term involves a parallel energy diffusion which if it doesn't play a dominant role is nonetheless essential to insure the non violation of the physics principles. Finally the last term is the pitch angle scattering of the ions which efficiently connects the parallel velocity direction with the perpendicular's one. As a remainder, for resonant ion velocity in the range $v_{thi} \ll v_{res} \ll v_{the}$, the ion-ion collisions provide a diffusion and a small drag while the ion-electron collisions provide only a drag. The classical expression for $C(f)$ is as follows :

$$C(f) = -\frac{1}{v^2}\frac{\partial}{\partial v}\left\{ v^2(\langle \Delta v_{//}\rangle + \frac{1}{2v}\langle \Delta v_{\perp}^2\rangle)\, f \right\} + \frac{1}{2v^2}\frac{\partial^2}{\partial v^2}\left\{ v^2\langle \Delta v_{//}^2\rangle\, f \right\} + \frac{1}{4v^2}\frac{\partial}{\partial \eta}\left\{(1-\eta^2)\frac{\partial}{\partial \eta}\left\{ \langle \Delta v_{\perp}^2\rangle\, f \right\}\right\}. \quad [27]$$

Here $\langle \Delta v_{//}\rangle$, $\langle \Delta v_{\perp}^2\rangle$, $\langle \Delta v_{//}^2\rangle$ are the classical diffusion coefficients induced by encounters of charged particles[30]. These coefficients are cumbersome but they depend only on the energy H and therefore are replaced by their expressions[7] in the formulas only at the last step.

The expression of L_{Coll} can now be derived after some simple but tedious algebra involving to perform a direct integration over Φ_2 for the terms of drag and of energy diffusion independent of Φ_2 and an integration by part for the others; to change variables $\{J_1,J_2\}$ to $\{h,p\}$ in the integration and $\{v,\eta\}$ to $\{h,p\}$ in $C(f)$. The expression of L_{Coll} takes two different forms depending upon the passing (P) and trapped (T) particle trajectories and it writes :

$$L_{Coll}^{P,T} = \int dp dh dJ_3\, \mathcal{J}^{P,T}\begin{bmatrix} J_1, p \\ J_2, h \end{bmatrix} \frac{m}{2h}\left\{ -\tilde{H}\, f'\partial_v^*[C_\alpha f] + \frac{\sqrt{\tilde{H}}}{2} f'\partial_v^*\partial_v^*[C_\beta f] \right\} + I_\eta^{P,T} \quad [28]$$

where : f is written in place of $\bar{f}$ because there is no ambiguity;

$$\mathcal{J}^P\begin{bmatrix} J_1, p \\ J_2, h \end{bmatrix} = \sqrt{\frac{m}{2}}\frac{qR_0}{\omega\sqrt{h+b(p-h)}};$$

$$\mathcal{J}^T\begin{bmatrix} J_1, p \\ J_2, h \end{bmatrix} = \sqrt{\frac{mR_0}{br_g}}\frac{qR_0}{\omega\sqrt{h-p}};$$

$$C_\alpha = \frac{2h}{m}\left(\langle \Delta v_{//}\rangle + \frac{1}{2}\sqrt{\frac{m}{2\tilde{H}}}\frac{1}{\sqrt{h}}\langle \Delta v_{\perp}^2\rangle \right);$$

$$C_\beta = \frac{2h}{m}\langle \Delta v_{//}^2\rangle;$$

and $\partial_v^* = \sqrt{2mh}\frac{\partial}{\partial h} + p\sqrt{\frac{2m}{h}}\frac{\partial}{\partial p}$.

For the last term resulting from the integration in pitch angle, the following expressions are obtained :

$$I_{\eta}^{P} = \sqrt{\tilde{H}} \int dp dh dJ_3 \frac{qR_0}{\omega} \sqrt[3/2]{\frac{m}{2}} \frac{p-h}{bh} \sqrt{h+b(p-h)} \langle \Delta v_{\perp}^2 \rangle \frac{\partial f}{\partial p} \frac{\partial f'}{\partial p} \qquad [29]$$

$$I_{\eta}^{T} = \sqrt{\tilde{H}} \int dp dh dJ_3 \frac{mqR_0}{2\omega b} \sqrt{\frac{mR_0}{r_g}} (p-h) \sqrt{\frac{h+b(p-h)}{h}} \langle \Delta v_{\perp}^2 \rangle \frac{\partial f}{\partial p} \frac{\partial}{\partial p} \left(\sqrt{\frac{h+b(p-h)}{bh(h-p)}} f' \right) \qquad [30]$$

IV. STEADY STATE SEMI ANALYTICAL f(h,p) SOLUTION

The functional L reduces to $-L_{QL} - L_{Coll}$ in the steady state case. Even so, it is a difficult task to find the solution in f over the all plasma and that necessitates to use powerful numerical algorithms. However the variational formulation leaves some degree of arbitrariness in the choice of the trial function depending upon what phenomenon is emphasized. In the present case the arbitrary degree is even greater as L_{QL} is made extremal by any function of p. This comes from the fact that the RF lines of diffusion which are the p = cst lines. But this apparent degeneracy is overcome by collisions which bring diffusion and drag and therefore make the particle exploration of the {h,p} domain possible. So in a first step a semi analytical solution is preferable as it will capture most of the physics and will serve as a guideline for latter numerical checks

The semi analytical modelling of f(p,h) aims at the determination of f(p,h) over one magnetic surface by means of variations of L. The adiabatic barrier is modelled by imposing the QL diffusion coefficient to be zero for $H \geq H_{Lim}$. The value of H_{Lim} corresponds to the adiabatic energy limit consistent with the chaotic behaviour study. However H_{Lim} is left as a free parameter which in turn allows to evaluate the influence of the Hamiltonian character of the interaction relative to the influence of collisions. Finally the RF field amplitude is an input of the model taken for a given heating situation from the predictive ALCYON numerical code[31].

Within the domain of quasi linear diffusion ($0 \leq P \leq H_{Lim}$) the choice of the f(p,h) form is free. So in order to account for the anisotropy and the collisional thermalisation, a representation with three parameters has been selected :

$$f(h,p) = \Lambda \left[\exp\left(-\frac{h}{t_0}\right) + \alpha\ p \exp\left(-\frac{p}{\Delta p}\right) \exp\left(-\frac{h}{t}\right) \right] \qquad [32]$$

where $t_0 = T_0/\tilde{H}$ and T_0 is the temperature of the bulk resonant population; Δp the characteristic anisotropy width in the p-direction; t the characteristic width in h due to the collisional drag. The parameter α represents the ratio of the accelerated to the bulk ions while Λ is not a free parameter as it insures the particle conservation.

If the trial function f' is chosen among the class of f-functions with a set of parameter $\{\alpha',\Delta p',t'\}$ then variations of L with respect to each f'-parameters leads to a system of three equations in α, Δp, t : the first two allows to derive Δp and t by means of a numerical solution and the other gives $\alpha(\Delta p,t)$.

A simulation is conducted for the minority hydrogen heating scenario in a typical TORE SUPRA (TS) plasma discharge with parameters listed in Table III. The RF frequency is set to 68 MHz which locates the resonant surface close to the plasma centre. From the output of the ALCYON code the RF power deposition profile is derived and appears localized inside the volume limited by a minor radius of 40 cm. The predicted RF power thermally absorbed by the hydrogen ions reaches 1.2 MW. The magnetic surface that is considered in the present modelling is set to $r_g = 25$ cm and the adiabatic energy barrier is set to 2 MeV. The slowing down time on electrons reaches 84 ms and to reproduce the predicted absorbed energy of 1.2 MW requires an electric field amplitude of 13 V/cm which is in the range of value predicted by ALCYON. This leads to a quasi linear energy $\tilde{H}$ of 73 eV. The semi analytical solution is then : a width ΔP equal to 66 keV ($\Delta P = p\tilde{H}$), T = 183 keV ($T = t\tilde{H}$) and a number of particle in the tail distribution reaching 3.3% of the total minority population. This is very different from what an isotropic simulation would produce for the tail temperature. In the Stix simulation[7] a tail temperature of 70 keV is found. The shape of the projection of f(h,p) along the energy vector is represented in Fig.12. A typical deep in the distribution function shape due to the anisotropy may be observed at $H \approx 50$ keV. A "negative" temperature behaviour may here be recognized, which needs to be compared with an experimental observation made in the Princeton Large Torus[32].

An horizontally scanning neutral charge-exchange analyser was mounted on PLT for the purpose of measuring, in the equatorial plane, the minority distribution function at four different sight angles ranging from parallel to perpendicular. At a certain angle and for particles moving in the co-direction, it was observed that the distribution

function exhibited a negative temperature behaviour. This was associated with the place along the trajectory where charge exchange occured, trapped particles weighting differently on the recorded signal than passing particles. So it was concluded that the negative temperature behaviour was the result of the anisotropic QL diffusion, but only through a geometrical effect. A simulation along this line was tentatively tried latter using a bounce averaged Fokker Planck code[33] in which the anisotropy of the distribution function is negligible. In order to simulate that behaviour it was required to adjust the power deposition profile to an extent which weakened the geometrical argument. So this must be viewed as an indication that the effect of trajectory is not fully responsible for the anormal distribution slope and consequently that the opposite argument of a strong anisotropic distribution function is partly supported by the reported experiment. If we introduce in our semi analytical model the parameter set of this experiment (D(H) plasma with 1% n_H/n_e, $E \approx 15$ V/cm, $r_{cH} = 7$ cm, $n_{c0} \approx 3\ 10^{19}$ m^{-3}, $T_{c0} = 1.1$ keV, $T_{i0} = 1.5$ keV) and try to simulate the experimental signal at different sight angles (Fig.13) we observe a good coherence between theory and experiment : the energy turning point occurs at 30 keV, the negative temperature effect is maximum for mid angle lines of sight and along the parallel direction the distribution function remains Maxwellian. However due to a functional dependence in p (or $v_{//}$) of the form pe^{-p} in the trial function there remains a small residual tail signal amplitude in the simulated parallel direction signal. Its amplitude is 100 dB lower than the corresponding perpendicular tail signal and to be observed experimentally, would require a dynamics range that is unachievable to date. This therefore does not contradict the experimental observation. In the case of an ^3He minority heating scheme[32] the energy turning point disappears (Fig.14) as experimentally observed. That is mainly due to the higher bulk ion temperature.

Further observations of the semi analytical simulations shows that for low temperature low collisionality plasmas the Δp-value is always very different from the t-value. This shows that there is some meaning to the functional form of the trial function and that anisotropy is effective. More generally two distinct regimes can be underscore depending upon the relative influence on the solution of adiabatic barriers or of collisions. The regime is collisional when the collisional drag is strong enough so that it prevents the particle energy from reaching the adiabatic limit. This regime is characterized by value independent of H_{Lim} and for a given experiment it is predominently influenced by a

relatively high electronic density. This is examplified in figure 15 for a typical TS discharge (Cf. Table III) for $n_e = 5.5\ 10^{19}\ m^{-3}$. The ICRF wave spectrum contains a single toroidal mode and the coupled RF power is set to 1.2 MW by adjusting the value of the RF electric field. Saturated width values in excess of 60 and 180 keV are respectively found for t and Δp. On the opposite for lower densities the solution enters the Hamiltonian regime characterized by a linear variation with H_{Lim} of the parameter Δp and t. Figure 16 shows this behaviour for a typical discharge of the Joint European Torus (JET) (Table IV) with : $n_e = 3.3\ 10^{19}\ m^{-3}$, 10 MW of coupled ICRF power and a magnetosonic wave with a single toroidal mode. The adiabatic barrier effect is beneficial as if it limits the Δp and t values, it also confines the particle population in a lower energy range. The range of H_{Lim} values being characteristic of what can be expected (Cf. for α-particles with a single toroidal harmonic H_{Lim} reaches a value of 800 keV), the adiabatic barrier effect should be observed in JET as the ICRF coupled power is increased. The advantage of confining the resonant particles in the few hundred keV range may benefit JET in studying the α-particle behaviour in the reactor environment. Indeed the energy reached by the ^3He particles is in the range where the cross section of the $(D,^3He) \rightarrow (^4He,p)$ reaction is maximum. Finally when H_{Lim} is further increased the Hamiltonian regime ends and a collisional behaviour of Δp and t is recovered. This may occur if the launched magnetosonic wave has many toroidal components which help rejecting the adiabatic limit to higher values.

V. CONCLUSIONS

The subject of concern of the present article has been to address the question of the ICRF heating dynamics in Tokamak plasma. In order to account for the fundamental anisotropy associated with the magnetosonic wave absorption, the problem has been analysed in the Hamiltonian frame where the integrable nature of the unperturbed particle trajectory can be given a simple form, when expressed in the canonical action angle variables. The QL nature of the RF induced diffusion has been studied and en passant the QLT has been validated by collisions or intrinsic stochasticity depending upon the temperature or the density. The Fokker Planck equation has then be given a variational form suitable to study the stationary distribution function of resonant ions. In the minority heating scenario and for a given magnetic surface, a semi analytical modelling of the Fokker Planck equation solution has been devised. This model has allowed to demonstrate that the heating dynamics was driven by the anisotropic nature of the RF power absorption and, when collisions are negligible, by the existence of an Hamiltonian regime in which adiabatic barriers limit the excursion in energy of the resonant ions. This regime appears to lower the averaged energy of the resonant ion tail and seems to prevail in Tokamaks like JET. This may benefit JET in the forthcoming α-particle simulation experiments where a quantitative fraction of the ^3He particle needs to be accelerated to energies in the 1 MeV range. Finally, the variational formulation of the Fokker Planck equation makes it suitable for computer handling and this work will find a natural continuation in the development of a finite element numerical code which will be linked to the existing 2D ICRF power deposition code ALCYON.

ACKNOWLEDGEMENT

The authors are grateful to Dr. D. Escande and Dr J-M. Rax for fruitful discussions.

APPENDIX

The state of a given system is specified by the set of variables $\{p_i\}$ and the density of probability to find the system in a state $\{p_i\}$ at a given time (t) is represented by a function of the t and p_i's variables : $f(p_i;t)$. The evolution of the density of probability $f(p_i;t)$ is governed by the master equation which involves a probability per unit time $W(p_i;p_i')$. $W(p_i;p_i')$ is a transition probability that the system transits from one state $\{p_i\}$ to another $\{p_i'\}$. From the master equation the Fokker Planck equation may be deduced if the two following conditions are realized: the reciprocity relation[34] holds so that $W(p_i;p_i') = W(p_i';p_i)$ and the changes in the set of p_i's variables take place in small jump so that $W(p_i;p_i')$ is a rapid decreasing function of the distance between two states[35] (the distance being defined in a vectorial space built out of the p_i's variables set). The Fokker Planck equation then takes the following form for continuous states :

$$\frac{\partial f(p_i;t)}{\partial t} = \frac{1}{2}\frac{\partial}{\partial p_i}\left(\langle \Delta p_i \Delta p_j \rangle \frac{\partial f(p_i;t)}{\partial p_i}\right) \qquad [33]$$

where $\langle \Delta p_i \Delta p_j \rangle = \int \Delta p_i \Delta p_j \, W(p_k;p_k') \, dp_k'$.

The Coulomb collisional operator $\mathcal{C}(f)$ may be written in the form of the RHS of Eq.[33] if the discussion is restricted to the Coulomb logarithmic accuracy. In this case the transition probability density is expressed in terms of a linear function of both the relative velocity of the two colliding particles and of the collision cross section[36].

In the case of the ICRF wave particle interaction, the RF diffusion operator may be derived from the Vlasov equation. When the Hamiltonian H is defined, then the action angle variables $\{J_k,\Phi_k\}$ are derived through the set of the Hamilton's equations (k=3 in our case). So it is possible to write the Vlasov equation in terms of the Poisson operator $\mathcal{H}$:

$$\frac{\partial f}{\partial t} = -\mathcal{H}(f) \qquad [34]$$

while $\mathcal{H}$ involves the canonical action angle variables : $\mathcal{H} = \sum_k \left(\frac{\partial H}{\partial J_k}\frac{\partial}{\partial \Phi_k} - \frac{\partial H}{\partial \Phi_k}\frac{\partial}{\partial J_k} \right)$

The quasi linear theory amounts to consider that the wave particle interaction is a perturbation of first order for the particle motion and of second order for the density of probability. Therefore the Hamiltonian is written $H = H_0(J_k) + \delta_1 H$ where the J_k's are the canonical actions derived from H_0 and are constants of the unperturbed motion. The density of probability is written $f = f_0(J_k) + \delta_1 f + \delta_2 f$, where $\delta_1 f$ is the linear plasma response to the RF perturbation. The perturbations $\delta_1 H$, $\delta_1 f$ are decomposed over the phases Φ_k, canonically conjuguated with the J_k's, and their expressions write :

$$\{\delta_1 H(J_k,\Phi_k,t),\delta_1 f(J_k,\Phi_k,t)\} = \sum_{N_n} \{h_{N_n}(J_k),f_{N_n}(J_k)\} \exp i(N_n\Phi_n + \omega t) + c.c. \quad [35]$$

while the first order Vlasov equation allows to derive the linear solution :

$$f_{N_n} = \frac{h_{N_n} N_k \frac{\partial f_0}{\partial J_k}}{\omega + N_k\omega_k + i\varepsilon}.$$

If we now consider the angle-averaged Vlasov equation as the evolution equation for the angle-averaged density of probability $\bar{f}(J_k,t) = \int \frac{d^3\Phi_k}{(2\pi)^3} f(J_k\Phi_k,t)$, then we may demonstrate that the time evolution equation for $\bar{f}$ is :

$$\frac{\partial \bar{f}}{\partial t} = \frac{1}{2}\frac{\partial}{\partial J_i}\left([4\pi \sum_{N_k} N_i N_j |h_{N_k}|^2 \delta(\omega + N_k\omega_k)] \frac{\partial \bar{f}}{\partial J_i} \right) \quad [36]$$

The presence of the delta function in the RF quasi linear diffusion operator shows the very strong influence of resonant trajectories. However this resonance localisation effect can be levelled down by chaos. In the case of chaos induced by intrinsic stochasticity this requires the resonance surfaces to be sufficiently dense so that the coefficients h_{N_k} have a weak dependence in N_k's. Then the summation just acts over the delta function and may be replaced by the inverse of the averaged distance $\delta\omega$ in between two close resonant surfaces when counted in $\{\omega_k\}$. In the case of minority ICRF heating with one toroidal mode that summation reduces to $1/\omega_2$.

TABLE I : action-angle variables for deeply passing and trapped particles (index 0 for value on the magnetic axis, Φ_T toroidal magnetic flux function, $\bar{\theta}$ maximum amplitude for trapped particle ($\theta = \bar{\theta}\sin(\phi_2)$), $\mathcal{J}_0$ zeroth order Bessel function).

Passing particle	Trapped particle
$J_1 = -\frac{m}{e}\mu\ ;\ \omega_1 = -\frac{eB_0}{m}\ ;\ \phi_1 = \phi_c + \frac{r_g\omega_1}{R_0\omega_2}\sin(\theta)$	$J_1 = -\frac{m}{e}\mu\ ;\ \omega_1 = -\frac{eB_0}{m}\left[1 - \frac{r_g}{R_0}\mathcal{J}_0(\bar{\theta})\right]$
$J_2 = e\Phi_T(\frac{J_3}{e}) + qmR_0v_{//}\ ;\ \omega_2 = \frac{\omega_3}{q}\ ;\ \phi_2 = \theta$	$J_2 = \frac{1}{2}mR_0^2q^2\bar{\theta}^2\omega_2\ ;\ \omega_2 = \omega_b = \frac{v_\perp}{qR_0}\sqrt{\frac{r_g}{2R_0}}$
$J_3 = e\Psi_P + mR_0v_{//}\ ;\ \omega_3 = \frac{v_{//}}{R_0}\ ;\ \phi_3 = \phi$	$J_3 = e\Psi_P;\ \omega_3 = \omega_d = \frac{qmv_\perp^2}{2er_gR_0B_0}\ ;\ \phi_3 = \phi - q\theta$

TABLE II : characteristic frequencies $\nu = \omega/2\pi$ as functions of temperature for a helium-4 plasma with $B_0 = 4$ T, $q = 2$, $r_g = 0.5$ m, $R_0 = 2.5$ m, $\bar{\theta} = 1$ rd ($n_e = 10^{20}m^{-3}$, E = 100 V/cm).

		pass. part. [$v_{//}(\theta=0) = v_\perp(\theta=0)$]			trapped particles		
$v_{//}(\theta=0)$ (keV)	N_2	ν_1 (MHz)	ν_2 (MHz)	ν_3 (MHz)	ν_1 (MHz)	ν_2 (MHz)	ν_3 (MHz)
10	-276	- 30	0.02	0.04	- 25	0.02	0.003
800	-30	- 30	0.20	0.40	- 25	0.20	0.24
3500	-14	- 30	0.40	0.80	- 25	0.43	1.20

TABLE III : Typical plasma parameters of the TORE SUPRA tokamak.

$B_T = 4.5$ T	$R_0 = 2.5$ m	$n_{e0} = 5.5\ 10^{19}$ m^{-3}	$n_{H0} = 5\ 10^{18}$ m^{-3}	$n_{D0} = 5.0\ 10^{19}$ m^{-3}
$\nu_{RF} = 68$ MHz	$r = 0.7$ m	$T_{e0} = 2.5$ keV	$T_{H0} = 2.0$ keV	$T_{D0} = 2.0$ keV

TABLE IV : Typical plasma parameters of the JET tokamak.

$B_T = 3.0$ T	$R_0 = 3.0$ m	$n_{e0} = 3.3\ 10^{19}$ m^{-3}	$n_{H0} = 3\ 10^{18}$ m^{-3}	$n_{D0} = 3\ 10^{19}$ m^{-3}
$\nu_{RF} = 45$ MHz	$r = 1.2$ m	$T_{e0} = 4.0$ keV	$T_{H0} = 3.5$ keV	$T_{D0} = 3.5$ keV

REFERENCES

[1]T.H. Stix, R.W. Palladino, Phys. Fluids **3**, 641 (1960).

[2]M. Rothman, R. Sinclair, I. Brown, J. Hosea, Phys. Fluids **12**, 2211 (1969).

[3]TFR Group, J. Plasma Phys. **24**, 615 (1982).

[4]D.Q. Hwang et al., in *Plasma Physics and Controlled Nuclear Fusion Research* (Proc. of the 9th Int. Conf., Baltimore, 1982) IAEA, Vienna Vol.II, 3 (1983).

[5]J. Jacquinot , JET Team, Plasma Phys. and Cont. Fusion **30**, 1467 (1988).

[6]L.-G. Eriksson, T. Hellsten, D.A. Boyd, Nucl. Fusion **29**, 87 (1989).

[7]L. Spitzer, *Physics of Fully Ionized Gases* (Interscience, New York, 1956).

[8]C.F. Kennel, F. Engelmann, Phys. Fluids **9**, 2377 (1966).

[9]T.H. Stix, Nucl. Fusion **15**, 737 (1975).

[10]R. Giannella, V. Zanza, E. Barbato, G. Braco, S. Corti, D.J. Gambier, Nucl. Fusion **28**, 193 (1988).

[11]V.L. Vdovin, in *Heating in Toroidal Plasmas* (Proc. of the 2nd Joint Grenoble-Varenna Int. Symp., 1980) CEC, Brussels Vol.I, 555 (1980).

[12]D. Anderson, W. Core, l.-G. Eriksson, Nucl. Fusion **27**, 911 (1987).

[13]V.B. Krapchev, Nucl. Fusion **25**, 455 (1985).

[14]G.W. Hammett, *Fast ion studies of ion cyclotron heating in the PLT Tokamak*, PhD Diss., Princeton Univ., NJ, 1986.

[15]J. Scharer, J. Jacquinot, P. Lallia, F. Sand, Nucl. Fusion **22**, 255 (1985).

[16]W.G.F. Core, *A Solution of the ICRF Fokker-Planck Equation*, JET Rep. JET-P(85)30 (1985).

[17]D.J. Gambier, A. Samain, Nucl. Fusion **25**, 283 (1985).

[18]A.N. Kaufman, Phys. Fluids **15**, 1063 (1972).

[19]W.G.F. Core, Nucl. Fusion **29**, 1101 (1989).

[20]A.J. Lichtenberg, M.A. Lieberman, *Regular and Stochastic Motion* (Springer Verlag, New York, 1983).

[21]T.D. Kaladze, A.I. Pyatak, K.N. Stepanov, in *Heating in Toroidal Plasmas* (Proc. of the Fourth Int. Symp., Rome, 1984) Vol.I, 476 (1984).

[22]D.F. Escande, Phys. Rep. **121**, (1985) 165-261, North Holland Amsterdam.

[23]B.V. Chirikov, *Review of Plasma Physics* (Ed. Kadomsev, Consultant Bureau, New York, 1987).

[24]T.G. Northrop, *The Adiabatic Motion of Charged Particles* (Interscience, New York, 1963).

[25]R.G. Littlejohn, Phys. Fluids **27**, 976 (1984).

[26]L.B. Felsen, N. Marcuvitz, *Radiation and Scattering of Waves* (Prentice-Hall, New Jersey, 1973).

[27]V.E. Zakharov, V.I. Karpman, Soviet Physics, JETP **43**, 490 (1962).

[28]D.F. Escande, private communication.

[29]S.C. Chiu, Phys. Fluids **28**, 1371 (1985).

[30]S. Chandrasekhar, Rev. Mod. Phys. **15**, 1 (1943).

[31]D.J. Gambier, A. Becoulet, A. Samain, in *Theory of Fusion Plasmas* (Proc. of Joint Varenna-Lausanne Int. Work., Chexbres, 1988) ISPP, SIF Bologna, 537 (1989).

[32]R. Kaita, R.J. Goldston, P. Beiersdorfer et al., Nucl. Fusion **23**, 1089 (1983).

[33]G.W. Hammett, R. Kaita, J.R. Wilson, Nucl. Fusion **28**, 2027 (1988).

[34]J.Oxenius, *Kinetic Theory of Particles and Photons* (Springer Verlag, New York, 1986).

[35]L.E.Reichl, *A Modern Course in Statistical Physics* (University of Texas Press., 1980).

[36]E.M. Lifshitz, L.P. Pitaevskii, *Physical Kinetics* (Landau and Lifshitz "Course of Theoritical Physics" Vol.10, Pergamon Press, London, 1981).

FIGURE CAPTIONS

Fig.1 Island like structure in the (λ,φ)-space for a particle trajectory in a potential well (the dashed line represent the resonant surface centre $\Omega(J) = 0$).

Fig.2 Trajectories in the phase space for the Hamiltonian paradigm[10] when two resonant surfaces are close together but when the Chirikov parameter is only 0.5 (the distance in between the two resonant surfaces J_{R1} and J_{R2} is $\Delta\Omega_R$; the island width $\Delta\Omega_I$; the solid lines represent the resonant surface centres).

Fig.3 Same as Fig.2 but for a Chirikov parameter S of 1.0 which suffices to induce intrinsic chaos.

Fig.4 Projection of the guiding centre drift surface in the $\{r_g,\theta\}$-plane for passing and trapped particles. Localization the ion cyclotron resonant surface $\omega+\omega_{ci}=0$, circulating (1) and trapped trajectories intersecting the resonance surface (2) or not (3).

Fig.5 Evolution of the relative trajectory phase as the particle crosses the resonance: (1) the two saddle points are separated (corresponding to cases (1) and (2) of Fig.4); (2) and (3) the two saddle points are connected; (4) there is no saddle points (case (3) of Fig.4).

Fig.6 $\left|\delta h_{N_k}\right|$ variations as function of the angular distance of the cyclotron resonance to the trajectory tip.

Fig.7 Poincaré mapping of λ versus Φ_2 (the combination $\Phi_1 + N\Phi_3 + \omega t$ is kept fixed) for 500 keV α-particles, E = 25 V/cm and q = 1.5 : (a) one resonant family N = 20 ($N_2 = -4, -5$); (b) two resonant families N = 20 ($N_2 = -4, -5$) and 21 ($N_2 = -6$).

Fig.8 Lines of quasi linear diffusion ($\leftrightarrow$) in the canonical action space for a given toroidal mode (the points ($\bullet$) indicate the localisation of the unperturbed trajectory).

Fig.9 Examples of the reciprocity principle violation : (a) the particle leaves the resonant surface following a given diffusion line $\vec{N}_i = \{1,N_2,N\}$ and return along a different one $\vec{N}_{i+1} = \{1,N_2+1,N\}$; (b) the toroidal antenna spectra contains different N_3 and the particle may equiprobably pick a direction of diffusion $\vec{N}_{i\alpha}$ or $\vec{N}_{i\beta}$ within the set $\{1,N_2,N_3\}$.

Fig.10 Domain of the particle trajectory type in the $(W,\omega J_1)$-space and direction of RF diffusion. Trajectories exist only in domains [2] and [3] while the banana tip does not intersect the resonant surface $\omega+\omega_{ci}=0$ in the domain [2]. Domain [1] is non physical.

Fig.11 Lines of QL RF diffusion in the $(v_{//,0},v_{\perp,0})$-space. Localisations of the trapped and passing trajectory domains and of the asymptotic direction (bold lines)

Fig.12 Projection of the resonant ion distribution function along the energy direction.

Fig.13 Projection along different sight angles of the distribution function for a value of the "b" parameter sets to 0.915 : (a) perpendicular direction $\frac{v_\perp}{v_{//}} = \sqrt{\frac{b}{1-b}} \approx 3.3$; (b) mid direction $\frac{v_\perp}{v_{//}} = \sqrt{\frac{b}{2-b}} \approx 0.92$; (c) parallel direction $\frac{v_\perp}{v_{//}} \approx 0$.

Fig.14 Same as 13 but for an ^3He minority heating scheme in a deuterium plasma and with the following parameters : $T_{e0} \approx 1.6$ keV, $T_{i0} = 3.1$ keV, $n_{e0} = 3.9\ 10^{19} m^{-3}$, $n_{^3He}/n_e \approx 6\%$, $r_{c^3He} = 7$ cm.

Fig.15 Influence of the adiabatic barrier on the Δp and t value in the collisional regime.

Fig.16 Influence of the adiabatic barrier on the Δp and t value in the Hamiltonian regime.

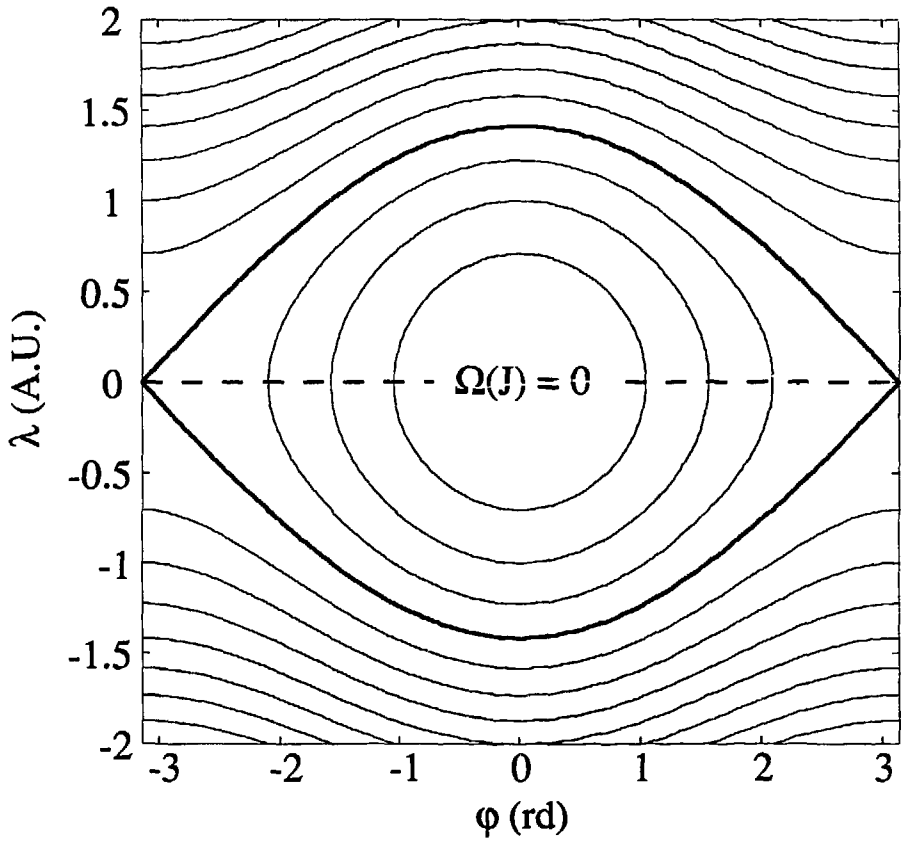

Fig.1

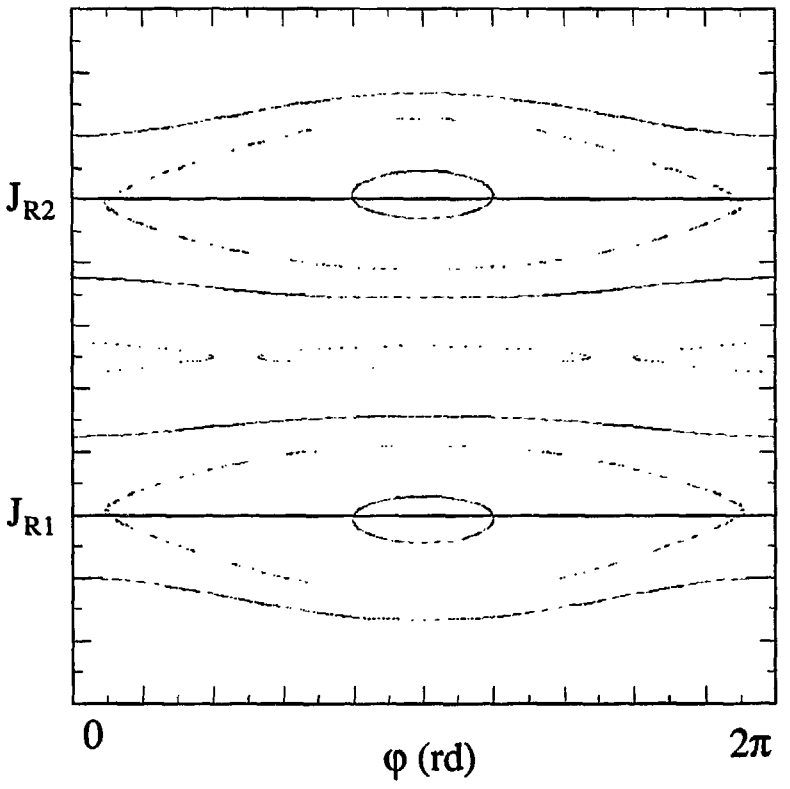

Fig.2

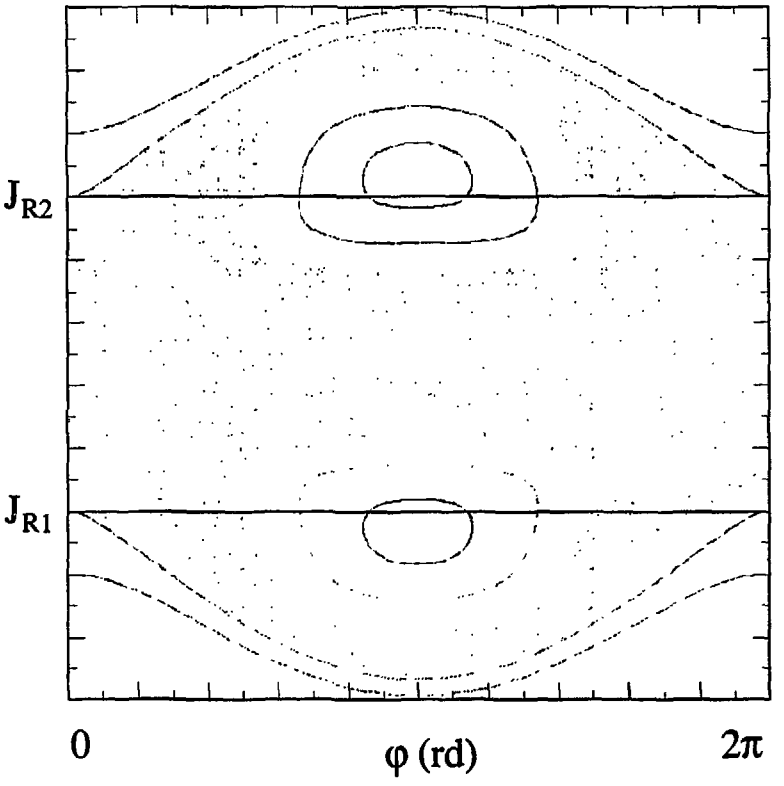

Fig.3

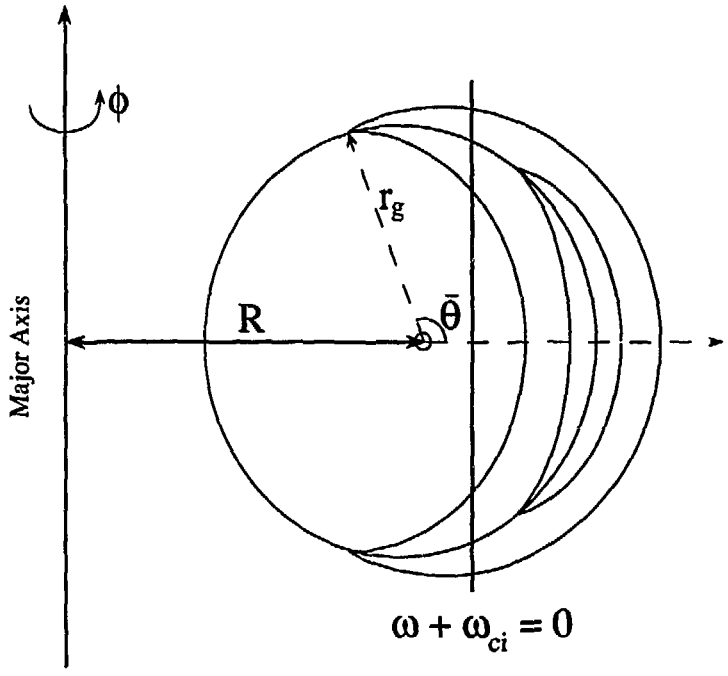

Fig.4

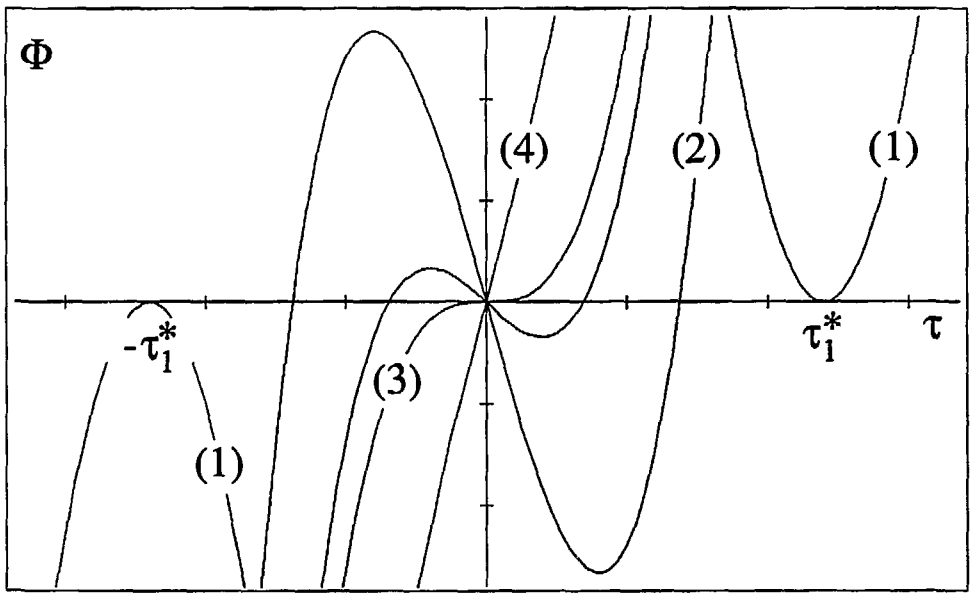

Fig.5

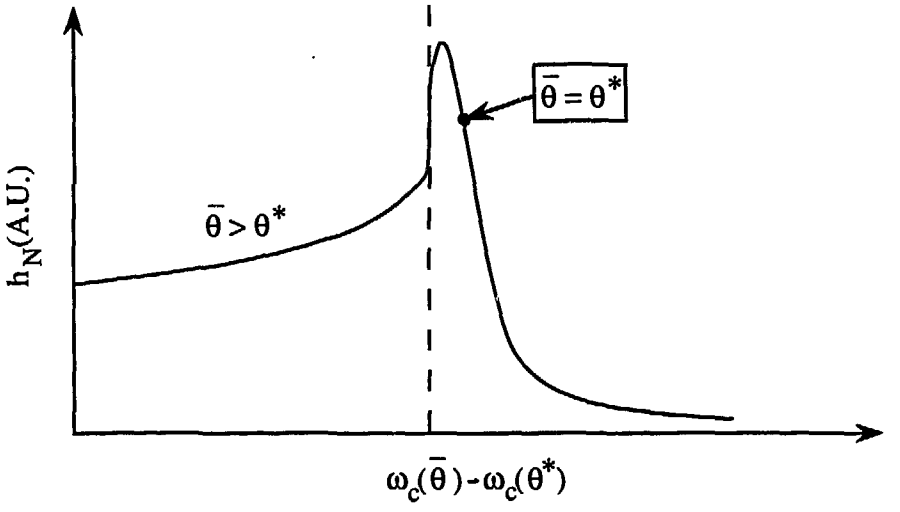
h_N(A.U.)
$\bar{\theta} > \theta^*$
$\bar{\theta} = \theta^*$
$\omega_c(\bar{\theta}) - \omega_c(\theta^*)$

Fig.6

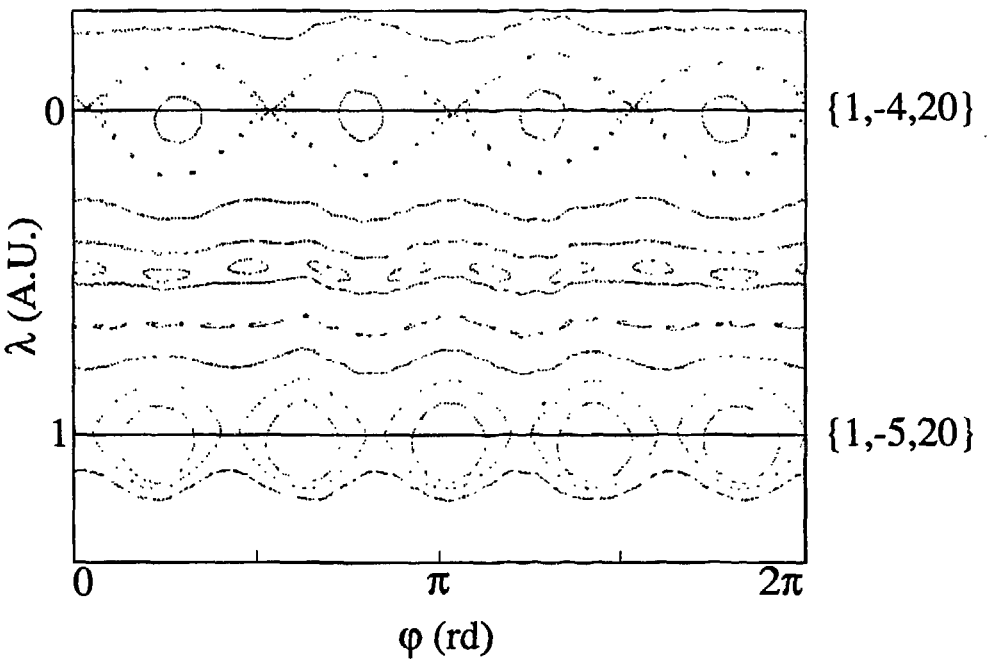

Fig.7-a

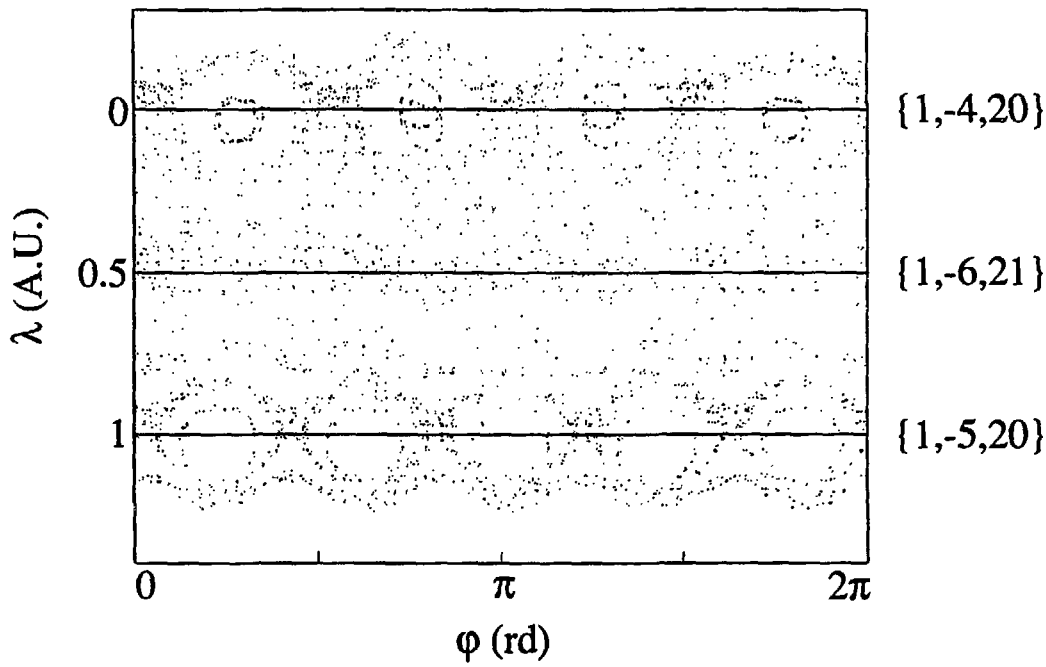

Fig.7-b

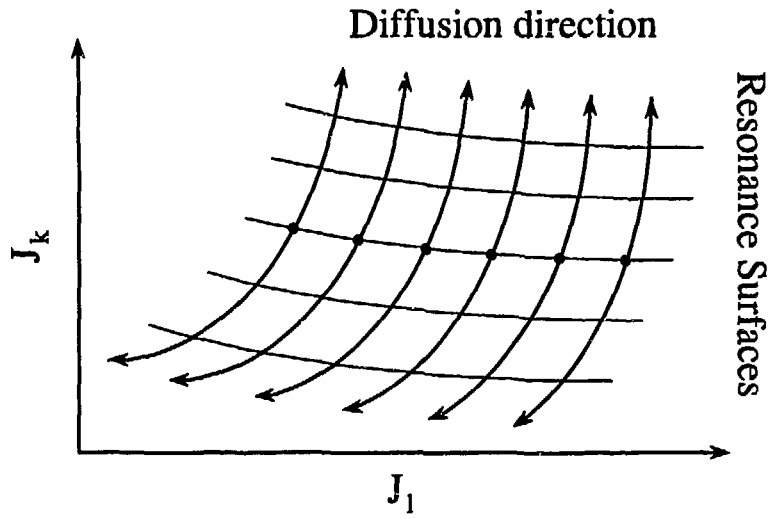

Fig.8

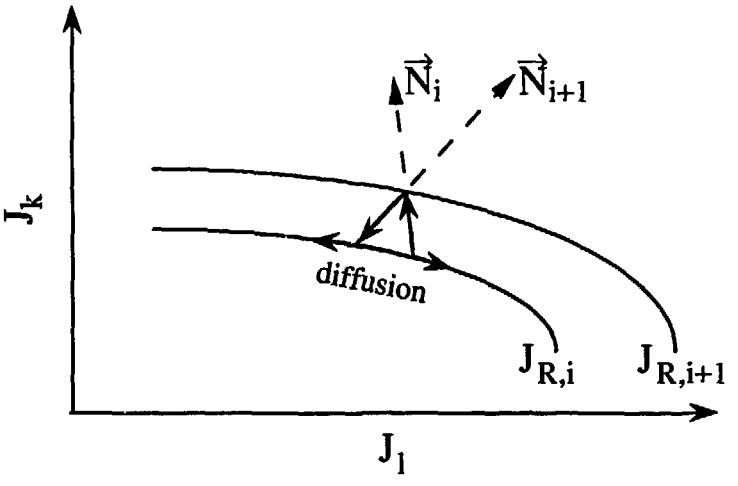
$\vec{N}_i$
$\vec{N}_{i+1}$
J_k
diffusion
$J_{R,i}$
$J_{R,i+1}$
J_l

Fig. 9-a

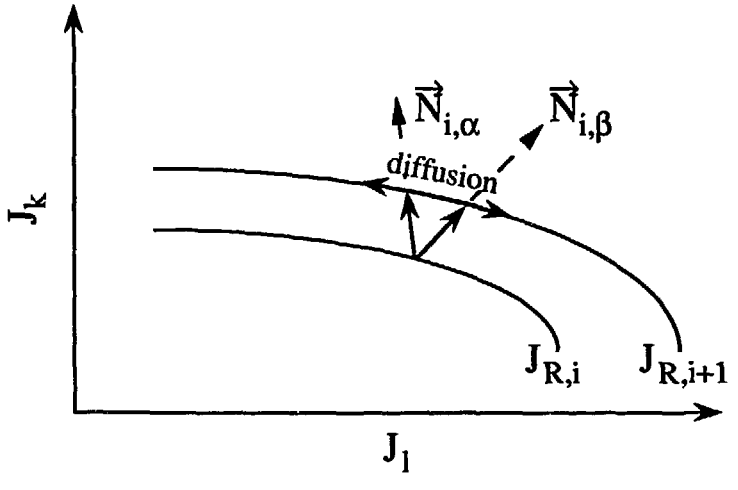
$\vec{N}_{i,\alpha}$
$\vec{N}_{i,\beta}$
diffusion
J_k
$J_{R,i}$
$J_{R,i+1}$
J_l

Fig. 9-b

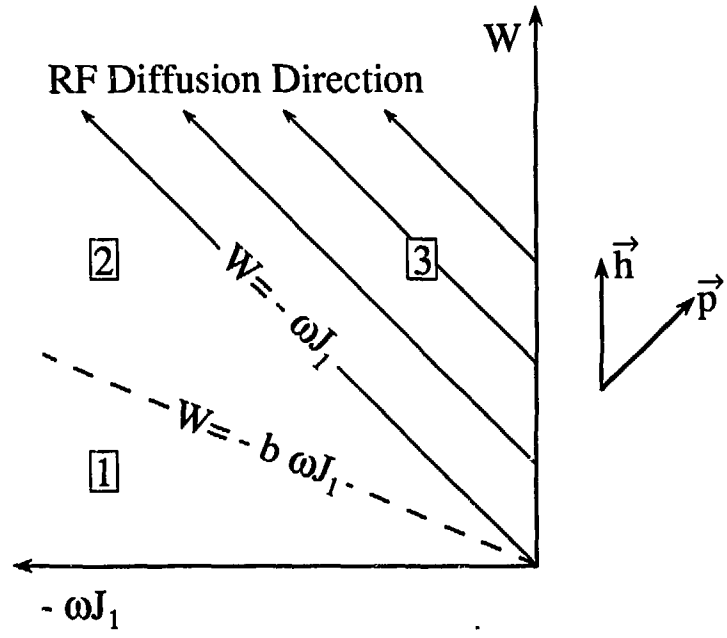
W
RF Diffusion Direction
2
3
1
$W = -\omega J_1$
$W = -b\,\omega J_1$
$\vec{h}$
$\vec{p}$
$-\omega J_1$

Fig.10

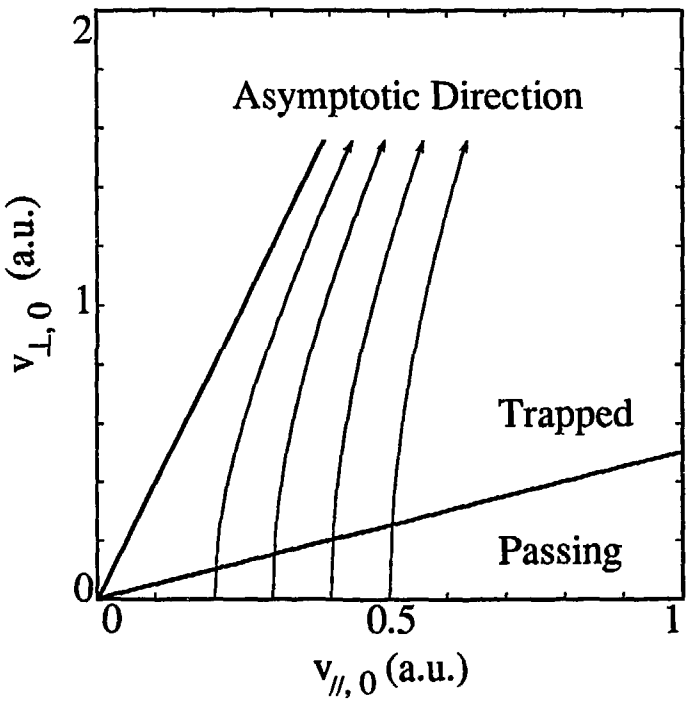
Asymptotic Direction
Trapped
Passing
2
1
0
0
0.5
1
$v_{\perp,0}$ (a.u.)
$v_{//,0}$ (a.u.)

Fig.11

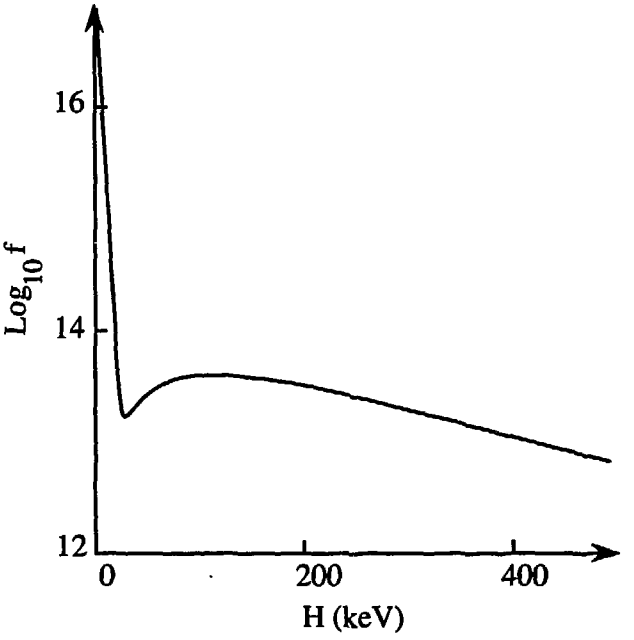

Fig.12

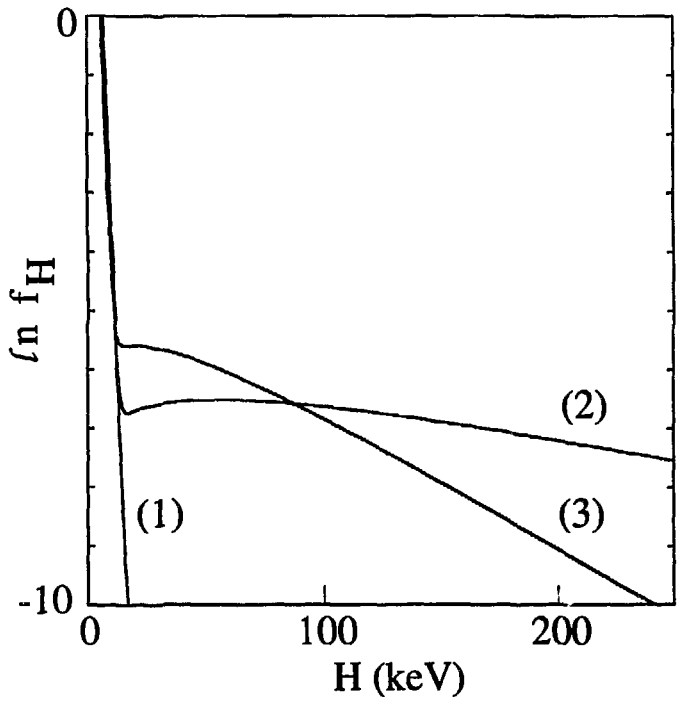

Fig.13

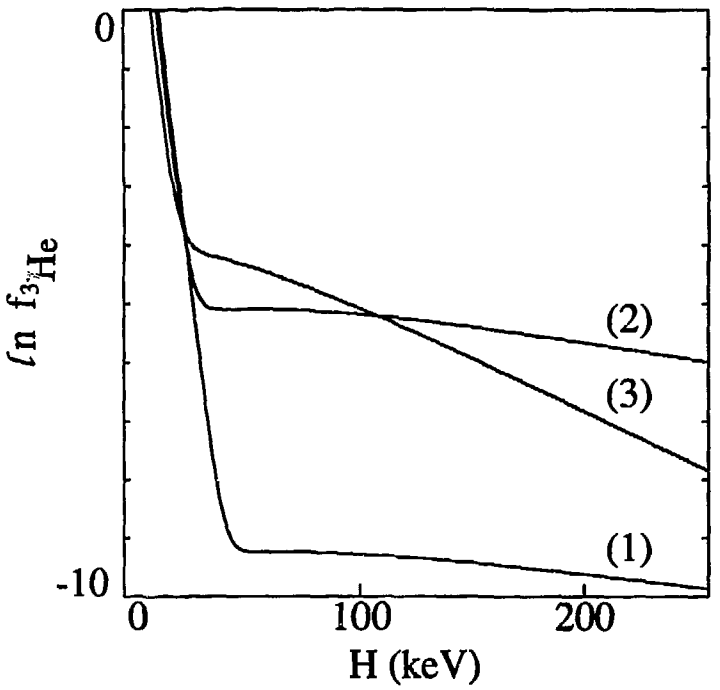

Fig.14

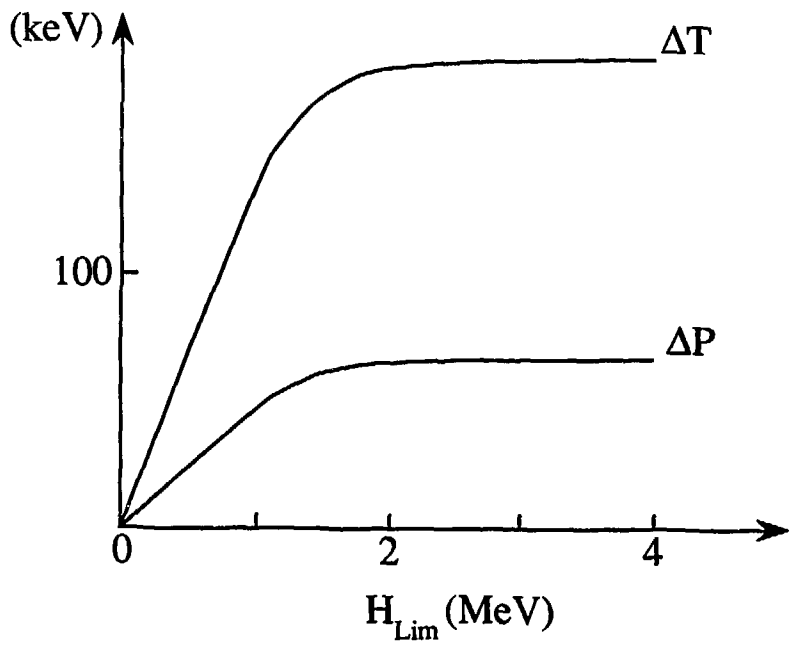

Fig.15

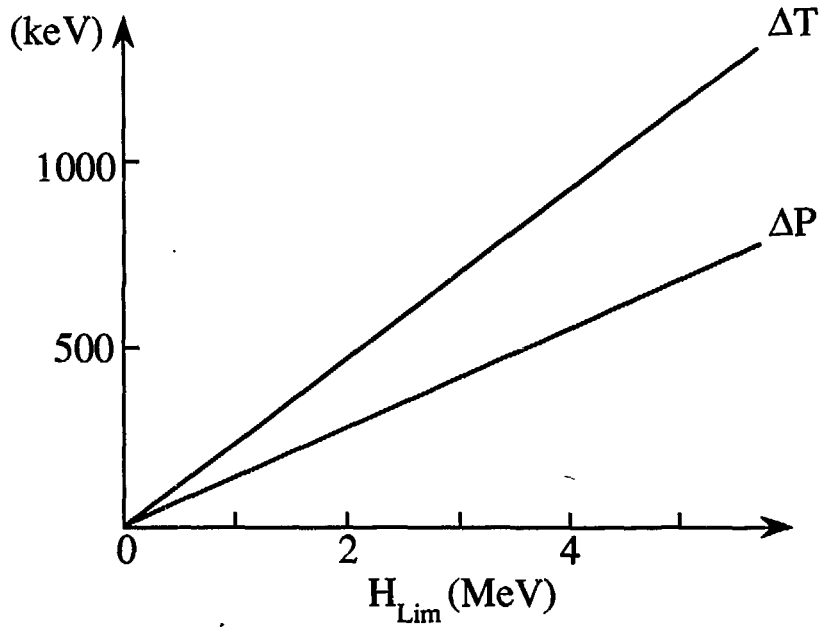

Fig.16